



## Techno-economic analysis of air-source heat pump (ASHP) technology for single-detached home heating applications in Canada

Artur Udovichenko & Lexuan Zhong

To cite this article: Artur Udovichenko & Lexuan Zhong (2020) Techno-economic analysis of air-source heat pump (ASHP) technology for single-detached home heating applications in Canada, Science and Technology for the Built Environment, 26:10, 1352-1370, DOI: [10.1080/23744731.2020.1787083](https://doi.org/10.1080/23744731.2020.1787083)

To link to this article: <https://doi.org/10.1080/23744731.2020.1787083>

 View supplementary material [↗](#)

 Published online: 07 Jul 2020.

 Submit your article to this journal [↗](#)

 Article views: 55

 View related articles [↗](#)

 View Crossmark data [↗](#)



# Techno-economic analysis of air-source heat pump (ASHP) technology for single-detached home heating applications in Canada

ARTUR UDOVICHENKO and LEXUAN ZHONG\*

*Department of Mechanical Engineering, University of Alberta, 9211-116 street NW, Edmonton, AB, T6G 1H9, Canada*

The air-source heat pump (ASHP) is a popular system that does not see much use in cold-climates despite its high potential in low carbon footprint. This study was designed to evaluate the techno-economic feasibility of its application to single-detached homes in Canada. First, a set of support vector regression (SVR) models was developed by a housing database for prediction of the exposed surface areas of homes in five Canadian cities: Vancouver, Toronto, Montreal, Edmonton, and Yellowknife. The predicted areas were then used to estimate the heat demands of all homes. As a result, the technical evaluation was conducted by comparison of the heat loss rate with the heat supply rate of ASHPs. Annual energy consumption was calculated using a bin method for furnace-alone and furnace/ASHP hybrid systems. Seasonal operating costs and greenhouse gases (GHG) emissions were estimated by utility costs and emissions factors for each city. Our findings show that Vancouver, Toronto, and Montreal are technically feasible to adopt the ASHP technology for economic and low GHG emission benefits. Although currently Edmonton and Yellowknife could not theoretically gain ASHP's benefits, the ASHP technology is still a promising technology to be implemented in the future if renewable energy infrastructures are established.

## Introduction

In 2016, residential energy consumption accounted for 17% of Canada's Secondary Energy Use, 60% of which came from space heating demand (Natural Resources Canada 2016). In most Canadian homes, natural gas furnaces are used to provide heating, as that is currently the most reliable and inexpensive source of energy. Although natural gas furnaces have become efficient, they possess greenhouse gas (GHG) emission issues. Thus, it is desirable to utilize clean energy heating systems. Air-source heat pump (ASHP) technology is the ideal candidate for this task, given that it is very practical in many mild-climate places, such as Saudi Arabia and Italy (Alshehri et al. 2019; Grossi et al. 2018). However, this technology is not as common in cold regions, due to ASHP efficiency decrease with outdoor temperature and frost accumulation on the evaporator-side heat exchanger (Bertsch and Groll 2008). As a result, the ASHP systems

hardly supply enough heating loads of residential buildings in cold climates.

The performance of ASHPs has been widely studied to better understand their limitations for generating potential solutions. A thorough review of the research was performed to cover various components, such as the use of an ejector, oil-injected compressor, and R-32/CO<sub>2</sub> refrigerant combinations, for the purpose of heating homes in the cold climate (Zhang et al. 2018). Other research has focused on the frosting effects of outdoor heat exchangers (Yao et al. 2004; Wang et al. 2013; Song et al. 2016, 2017). Furthermore, some innovations such as surface treatments (Jhee, Lee, and Kim 2002), spray solutions (Jiang et al. 2014), and solid desiccants (Zhang, Fujinawa, and Saikawa 2012) have been explored to solve the issues. Moreover, the development of a frost-free ASHP (Wang et al. 2017; Wang et al. 2018) and other setups with supplemental systems has been achieved (Guoyuan, Qinhu, and Yi 2003; Jin et al. 2016; Zhang et al. 2016; Huang and Hewitt 2013). Alternatively, 'solar-assisted' ASHPs, which are supplemented with solar collectors to enhance heat transfer on the evaporator side, have been tested in the cold regions of China (Long et al. 2019; Liu et al. 2017; Luo et al. 2017). However, studying the specific components and performance of ASHPs is not the only perspective for addressing limitations for residential applications.

Received February 22, 2020; Accepted June 4, 2020

**Artur Udovichenko, BSc**, Student Member ASHRAE, is an MSc student. **Lexuan Zhong, PhD**, Member ASHRAE, is an Assistant Professor.

 Supplemental material for this paper is available online.

\*Corresponding author e-mail: [lexuan.zhong@ualberta.ca](mailto:lexuan.zhong@ualberta.ca)

Other research has focused on modeling the performance of the ASHP system and the building in which it is operated, with the intent of identifying potential energy savings of ASHPs. These include homes operated with an ASHP and supplemented with a photovoltaic (PV) collector (Kamel and Fung 2014), an ASHP and a furnace with on-site solar PV generation (Demirezen, Ekrami, and Fung 2019), an ASHP water heater (Amirirad, Kumar, and Fung 2018); all in Ontario. Additionally, 20 net-zero or nearly-net-zero energy homes operated in New England, some of which incorporated ASHPs (Thomas and Duffy 2013), an apartment building numerically simulated with a heat recovery ventilator (HRV) and ASHP under the conditions of several Canadian cities (Li, Wild, and Rowe 2019), and a commercial building simulated and experimentally tested with an ASHP in Tibet to study the effect of high altitude (Li et al. 2017).

Although such efforts have been made to expand the potential application of ASHP technology in cold regions, most of the studies were based on specific building features and climatic conditions. Thus, the results may not be applicable to diverse building construction and varying locations. This absence of a broad view of technical feasibility and economic benefits of utilizing ASHP technology in the residential sector of cold climates may impede the improvement of market available ASHPs. In order to quantify the discrepancy between the energy demands of existing Canadian homes and the heat capacity of on-shelf ASHPs, the overall residential energy demand across Canada is necessary to be quantified.

Support vector regression (SVR) is known to be a very powerful modeling algorithm, which is based on developing a linear relationship with the use of nonlinear functions (Vapnik, Golowich, and Smola 1997; Parveen, Zaidi, and Danish 2019), constrained by carefully selected hyperparameters (Laref et al. 2019). SVR has been implemented and verified in some studies: forecasting building electricity load (Chen et al. 2017; Goudarzi et al. 2019), predicting building energy consumption based on outdoor conditions and various building characteristics (Wang, Lu, and Li 2019; Ma, Ye, and Ma 2019), and forecasting cooling load of a commercial building (Li et al. 2009; Xuan et al. 2019). In this paper, given the diversity of building architecture and envelope systems across Canada, SVR is a tool to predict building exposure areas that considerably influence energy loss.

The objectives of this study are: (1) to develop and train SVR models from a Canadian housing database for predicting the exposure areas of a random single-detached home in five Canadian cities: Vancouver, Toronto, Montreal, Edmonton, and Yellowknife; (2) to evaluate the technical feasibility of the ASHP technology in Canadian residential buildings by comparing the energy demands of homes with heat capacities of selected ASHPs; (3) to conduct economic and GHG emission analysis to quantify the differences between traditional furnace heating system and ASHP/furnace hybrid heating system; and (4) to predict GHG emission changes on a municipal level if half or all homes in each city adopt the ASHP technology. This study provides a clear statistical view of the applicability of the ASHP technology for five Canadian cities, which may help governing

organizations update building codes for energy-saving and facilitate HVAC manufacturers to improve ASHPs.

## Methodology

### *Canadian single-detached housing database*

House data used for this study was acquired from the Canadian Single-Detached and Double/Row Housing Database (CSDDRD) (Swan, Ugursal, and Beausoleil-Morrison 2009) that has proven to be useful in other studies (Di Placido, Pressnail, and Touchie 2014). The raw database lists various architectural, physical and geometric information about 16,952 Canadian homes of varying style, vintage and location in the country.

Through preliminary descriptive inspection of the database, it was found that the most common style of home in Canada can be described according to the characteristics listed in [Table A1 in the Supplemental Material](#). Given that more than half of all occupied dwellings in Canada are single-detached homes (Statistics Canada 2017), focusing on this style of home has relevant implications. The data was filtered to only include single-detached homes, and the data size was reduced from 16,952 to 10,075. Furthermore, due to some cases listing invalid or missing quantities that are relevant to heating load calculation in this study, the final total number of homes used for heating load analysis was reduced to 9,920.

Some calculations for the raw database were made to expand the necessary variables. For example, the exterior wall area was not explicitly stated in the data file, but other similar geometric parameters such as perimeter and wall height of each storey were included. The new variable of the gross exterior wall area was used in subsequent analyses and modeling procedures. The number of bedrooms was not a known parameter in the database, so it was approximated by considering the number of occupants instead under the assumption that one bedroom is equivalent to two occupants and any subsequent occupants occupy one bedroom. Other useful parameters listed in the database include plan shape, conditioned floor area, and footprint characteristics.

The plan shape is a categorical variable, which means that it takes numeric value to represent a characteristic that is entirely independent of the numeric value. In this case, it describes the shape of the house's footprint on grade, i.e. rectangular, T-shaped, L-shaped, or other complex layouts. The conditioned floor area includes the interior floor area of the residence above the ground. Also, the perimeters and areas of the house footprint refer to the measurements made on-grade and around the base of homes. Figure A1 presents a visual description of these variables in a sample home. It is crucial to note that all the data, organization, labeling, and any other details found in the files were assumed to be correct and legitimate.

### *Cluster analysis*

It has been assumed that houses built in different geographical locations during the past century will have different space heating energy demands due to varying outdoor conditions as well as construction standards and practices. To

Table 1. Cluster results for zone and year (vintage) bin.

	Zone 4				Zone 5				Zone 6				Zone 7				Zone 8			
	Year Bin	n	Mean	Std. Dev.	n	Mean	Std. Dev.													
Area of Footprint, m <sup>2</sup> (ft <sup>2</sup> )	1900–1938	13	127 (1377)	41 (442)	280	102 (1106)	46 (496)	243	93 (1010)	37 (408)	323	100 (1081)	77 (829)	N/A						
	1939–1971	58	119 (1287)	31 (343)	1320	121 (1303)	46 (505)	1305	109 (1179)	44 (476)	1048	110 (1189)	73 (786)	6	100 (1081)	8 (91)	6	100 (1081)	8 (91)	
	1972–2003	73	127 (1372)	43 (464)	1620	124 (1337)	41 (448)	2403	110 (1187)	38 (412)	1371	118 (1277)	40 (436)	12	89 (965)	33 (358)	18	89 (965)	33 (358)	
Total	144	124 (1338)	38 (416)	3220	121 (1303)	44 (480)	3951	109 (1174)	40 (436)	2742	113 (1220)	59 (645)	18	93 (1004)	27 (297)	N/A				
Perimeter of Footprint, m (ft)	1900–1938	13	50 (164)	10 (34)	280	42 (137)	9 (31)	243	40 (132)	8 (29)	323	40 (132)	10 (33)	N/A						
	1939–1971	58	45 (148)	6 (19)	1320	45 (148)	8 (28)	1305	42 (140)	7 (25)	1048	42 (139)	8 (27)	6	41 (135)	2 (7)	6	41 (135)	2 (7)	
	1972–2003	73	48 (159)	8 (27)	1620	45 (150)	8 (26)	2403	43 (141)	7 (24)	1371	44 (146)	7 (24)	12	38 (125)	7 (24)	12	38 (125)	7 (24)	
Total	144	47 (155)	7 (25)	3220	45 (148)	8 (27)	3951	42 (140)	7 (25)	2742	43 (142)	8 (27)	18	39 (128)	6 (20)	N/A				
Number of Bedrooms	1900–1938	13	2.2	1.1	280	2.4	1.2	243	2.3	1.0	323	1.9	1.2	N/A						
	1939–1971	58	2.4	1.3	1320	2.3	1.1	1305	2.2	1.2	1048	2.0	1.2	6	1.8	1.0	6	1.8	1.0	
	1972–2003	73	2.6	1.4	1620	2.6	1.1	2403	2.3	1.1	1371	2.2	1.2	12	0.8	1.1	12	0.8	1.1	
Total	144	2.5	1.3	3220	2.5	1.1	3951	2.2	1.2	2742	2.1	1.2	18	1.2	1.2	18	1.2	1.2		
Plan Shape (categorical)	1900–1938	13	5.2	2.2	280	3.6	2.0	243	3.5	2.0	323	3.6	1.8	N/A						
	1939–1971	58	4.1	1.7	1320	3.1	1.7	1305	3.0	1.6	1048	3.3	1.6	6	3.0	1.1	6	3.0	1.1	
	1972–2003	73	4.4	2.2	1620	3.7	2.1	2403	3.1	1.8	1371	3.8	2.0	12	4.3	2.3	12	4.3	2.3	
Total	144	4.4	2.0	3220	3.4	1.9	3951	3.1	1.7	2742	3.6	1.8	18	3.8	2.0	18	3.8	2.0		
Number of Floors	1900–1938	13	1.8	0.4	280	1.8	0.4	243	1.9	0.3	323	1.5	0.5	N/A						
	1939–1971	58	1.1	0.3	1320	1.2	0.4	1305	1.2	0.4	1048	1.1	0.3	6	1.0	0.0	6	1.0	0.0	
	1972–2003	73	1.5	0.5	1620	1.7	0.5	2403	1.4	0.5	1371	1.3	0.4	12	1.4	0.5	12	1.4	0.5	
Total	144	1.4	0.5	3220	1.5	0.5	3951	1.4	0.5	2742	1.2	0.4	18	1.3	0.5	18	1.3	0.5		
Conditioned Floor Area, m <sup>2</sup> (ft <sup>2</sup> )	1900–1938	13	204 (2203)	78 (849)	280	140 (1509)	56 (613)	243	140 (1515)	41 (450)	323	103 (1112)	32 (351)	N/A						
	1939–1971	58	127 (1375)	45 (484)	1320	120 (1293)	44 (476)	1305	111 (1198)	34 (376)	1048	101 (1090)	25 (270)	6	95 (1032)	8 (92)	6	95 (1032)	8 (92)	
	1972–2003	73	179 (1928)	67 (728)	1620	173 (1868)	58 (634)	2403	122 (1316)	41 (445)	1371	120 (1292)	33 (359)	12	106 (1145)	16 (177)	12	106 (1145)	16 (177)	
Total	144	160 (1730)	66 (716)	3220	148 (1601)	59 (635)	3951	119 (1289)	40 (431)	2742	110 (1194)	31 (341)	18	102 (1107)	14 (160)	N/A				
Gross Wall Area, m <sup>2</sup> (ft <sup>2</sup> )	1900–1938	13	215 (2322)	73 (792)	280	171 (1844)	52 (569)	243	167 (1806)	41 (451)	323	130 (1405)	38 (419)	N/A						
	1939–1971	58	135 (1454)	46 (499)	1320	128 (1386)	43 (472)	1305	119 (1285)	34 (370)	1048	109 (1173)	22 (247)	6	98 (1060)	5 (62)	6	98 (1060)	5 (62)	
	1972–2003	73	185 (1991)	61 (667)	1620	182 (1959)	52 (569)	2403	135 (1454)	46 (501)	1371	131 (1414)	41 (441)	12	137 (1480)	23 (255)	12	137 (1480)	23 (255)	
Total	144	167 (1805)	63 (684)	3220	159 (1714)	55 (598)	3951	131 (1420)	44 (475)	2742	122 (1321)	36 (393)	18	124 (1340)	27 (291)	N/A				
Basement Floor Area, m <sup>2</sup> (ft <sup>2</sup> )	1900–1938	13	115 (1240)	44 (477)	280	78 (849)	31 (334)	243	72 (779)	22 (243)	323	68 (740)	18 (203)	N/A						
	1939–1971	58	100 (1079)	29 (315)	1320	94 (1021)	28 (307)	1305	89 (967)	25 (275)	1048	88 (952)	21 (236)	6	89 (960)	7 (83)	6	89 (960)	7 (83)	
	1972–2003	73	111 (1198)	40 (440)	1620	99 (1074)	31 (333)	2403	88 (954)	24 (266)	1371	95 (1022)	24 (263)	12	82 (892)	25 (277)	12	82 (892)	25 (277)	
Total	144	107 (1154)	37 (400)	3220	95 (1033)	30 (329)	3951	88 (947)	25 (271)	2742	89 (962)	24 (261)	18	85 (915)	21 (230)	N/A				
Basement Wall Area, m <sup>2</sup> (ft <sup>2</sup> )	1900–1938	13	113 (1219)	29 (318)	280	76 (819)	20 (222)	243	71 (770)	19 (207)	323	73 (788)	15 (165)	N/A						
	1939–1971	58	102 (1108)	23 (251)	1320	93 (1002)	21 (230)	1305	89 (960)	19 (211)	1048	89 (962)	17 (183)	6	91 (986)	7 (85)	6	91 (986)	7 (85)	
	1972–2003	73	109 (1183)	27 (300)	1620	102 (1100)	21 (229)	2403	94 (1013)	18 (195)	1371	98 (1062)	18 (198)	12	91 (984)	20 (215)	12	91 (984)	20 (215)	
Total	144	107 (1156)	26 (284)	3220	96 (1035)	22 (243)	3951	91 (981)	19 (210)	2742	92 (991)	19 (208)	18	91 (984)	16 (179)	N/A				
Ceiling Area, m <sup>2</sup> (ft <sup>2</sup> )	1900–1938	13	128 (1377)	42 (456)	280	88 (952)	34 (366)	243	84 (913)	27 (292)	323	80 (871)	25 (273)	N/A						
	1939–1971	58	118 (1271)	27 (294)	1320	104 (1123)	31 (340)	1305	98 (1055)	26 (282)	1048	97 (1052)	34 (372)	6	95 (1032)	8 (92)	6	95 (1032)	8 (92)	
	1972–2003	73	126 (1357)	44 (477)	1620	111 (1201)	32 (346)	2403	97 (1048)	26 (282)	1371	107 (1154)	30 (330)	12	85 (915)	26 (284)	12	85 (915)	26 (284)	
Total	144	123 (1324)	38 (411)	3220	106 (1148)	32 (353)	3951	96 (1042)	30 (325)	2742	100 (1082)	32 (353)	18	88 (954)	22 (241)	18	88 (954)	22 (241)		

Note: n refers to the number of house records.

**Table 2.** Pearson correlation coefficient between inputs and outputs of SVR models. All correlation is significant at the  $p < 0.01$  level (2 tailed).

	Basement Floor Area	Basement Wall Area	Ceiling Area	Gross Wall Area
Perimeter of Footprint	0.645	0.578	0.622	0.252
Area of Footprint	0.536	0.445	0.520	0.189
Plan Shape	0.230	0.269	0.253	0.303
Conditioned Floor Area	0.487	0.416	0.522	0.898
Number of Bedrooms	0.082	0.103	0.070	0.171
Number of Floors	-0.239	-0.187	-0.149	0.812
Climatic Zone	-0.113	-0.099	-0.099	-0.298
Year Bin	0.165	0.306	0.146	0.126

group by zone, the house records were manually categorized based on the city they were built in, and which zone that city belonged to, resulting in five zone data subsets.

On the other hand, the years in which the homes were built did not have preassigned grouping criteria. So, the K-means cluster analysis was used to group all records into various numbers of vintage groups based on the year-variation of all housing parameters. Cluster number ranging from two to six was explored. In addition, the one-way ANOVA test was performed to select the best cluster number that showed the largest statistical significance of yearly variation, as well as to identify which housing parameters had significant variation throughout the years. IBM's SPSS software was chosen for this operation since it allowed the cluster membership numbers to be saved to the dataset, such that the groups were easily identifiable in subsequent analyses.

This procedure identified ten housing parameters that have statistically significant variation by the year the home was built, and it grouped housing records into three year-bins. A second ANOVA test was conducted amongst these unique variables by zone. Table 1 shows the numerical breakdown of the database used in this study by the fifteen unique year bin and zone scenarios. It also lists the descriptive statistics of the ten housing parameters identified as having variation by year and by zone.

### Support vector regression (SVR) model

#### Output selection

In order to estimate the energy requirements of large housing datasets without an architectural analysis of the engineering parameters of each residence, the SVR models were designed to predict the gross exterior wall area (above ground), ceiling area, and basement wall and floor areas of a random Canadian home. These exposure areas were defined as the SVR model outputs since the heat conduction through the building envelope systems dominate energy losses in cold regions and, most importantly, energy losses exhibit a linear relationship with the exposure areas. The fenestration areas were considered as targets for SVR modeling, but no significant relationships were identified during cluster analysis. Hence, during subsequent analyses, these parameters were obtained from the database directly.

#### Input selection

Ideally, the input parameters would have been almost entirely trivial and easy to describe a house. A two-tailed Pearson correlation test was conducted across the twelve variables displayed in Table 1 to determine how the four target variables are affected by the remaining eight. The correlations with the highest coefficients were prioritized for input selection. Table 2 shows that the perimeter and area of the house footprint have high and positive correlations with most of the target variables. Figure 1 shows the target variables and the inputs selected for the development of four SVR models.

#### Model training and evaluation

The model development procedures broke down as follows:

- Assignment of input and target variables listed in Figure 1. Each of the four models was executed separately; the same version of the MATLAB script was used for each run and only the one output variable was implemented.
- Division of the whole dataset into training and testing subset according to a random 80/20 split. The training set was used for development via optimization, cross-validation, and training. The test data set served as a final test to ensure that over-training had not occurred.
- Optimization of all hyperparameters based on the training subset. The parameters include box constraint (C), epsilon ( $\epsilon$ ), kernel function (Gaussian, linear, or polynomial), and polynomial order (only if kernel function = polynomial). This step was performed with the 'Bayesian' optimizer and with 10-fold cross-validation on the training subset.
- Training of the learner with the best observed (according to the algorithm) selection of hyperparameters on the training subset.
- Prediction of results in both training and testing data subsets.
- Evaluation of results in both data subsets by comparison with observed values according to the following performance measures: correlation coefficient ( $R^2$ ), mean absolute error (MAE), root mean squared error (RMSE), mean absolute percentage error (MAPE), and Willmott's index of agreement (WI).
- In order to generate a range of uncertainty in the result, the mean absolute error (MAE) of the testing subset of each model was propagated through the heating load

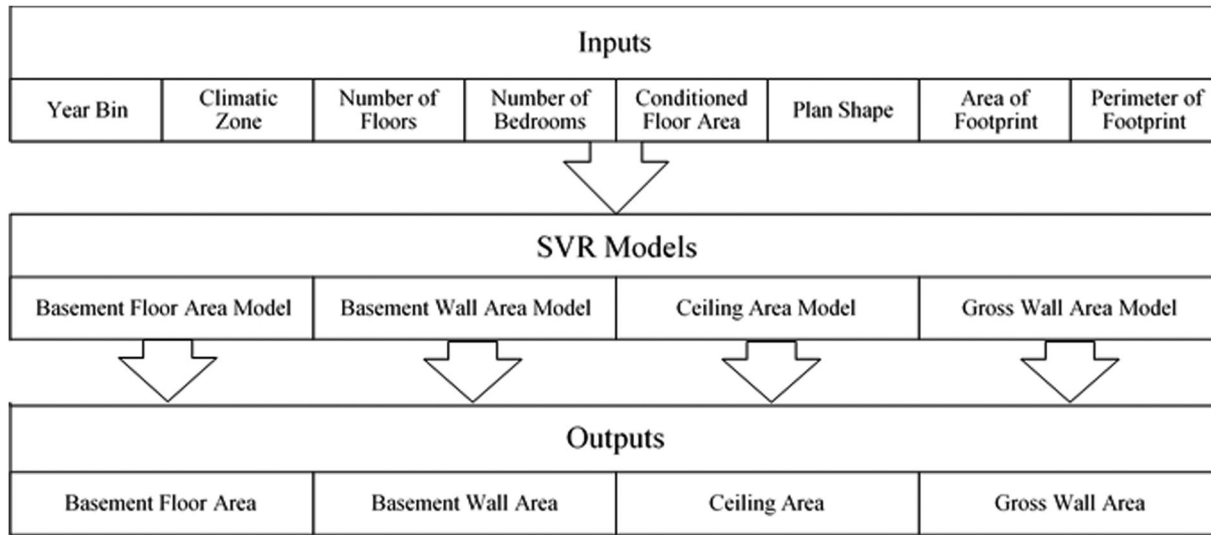


Fig. 1. Inputs and outputs of SVR models.

Table 3. Canadian cities used for analysis.

Location	Vancouver, BC	Toronto, ON	Montreal, QC	Edmonton, AB	Yellowknife, NWT
Climatic Zone <sup>a</sup>	Zone 4	Zone 5	Zone 6	Zone 7	Zone 8
Heating Degree Days @ 18.3 °C (65 °F) <sup>a</sup>	2911 (5240)	3518 (6333)	4146 (7463)	5198 (9423)	8159 (14687)
Heating Outdoor Design Temperature <sup>a</sup>	−3.4 °C (25.9 °F)	−13.7 °C (7.4 °F)	−19.2 °C (−2.5 °F)	−25.8 °C (−14.5 °F)	−38.3 °C (−36.9 °F)
Electricity Utility Rate <sup>b</sup>	0.10 \$/kWh (2.93 \$/therm)	0.10 \$/kWh (2.93 \$/therm)	0.06 \$/kWh (1.75 \$/therm)	0.12 \$/kWh (2.32 \$/therm)	0.29 \$/kWh (8.51 \$/therm)
Electricity Consumption Emission Factor <sup>c</sup>	10.9 gCO <sub>2</sub> /kWh (0.71 lbCO <sub>2</sub> /therm)	35.0 gCO <sub>2</sub> /kWh (2.27 lbCO <sub>2</sub> /therm)	1.6 gCO <sub>2</sub> /kWh (0.10 lbCO <sub>2</sub> /therm)	860.0 gCO <sub>2</sub> /kWh (55.8 lbCO <sub>2</sub> /therm)	267.5 gCO <sub>2</sub> /kWh (17.3 lbCO <sub>2</sub> /therm)
Electricity Generation Mix (% renewable)	89 %	93 %	99 %	9 %	37 %
Traditional Fuel Option	Natural Gas				Light Fuel Oil
Traditional Fuel Utility Rate	1.91 \$/GJ (0.22 \$/therm) <sup>d</sup>	3.66 \$/GJ (0.39 \$/therm) <sup>d</sup>	3.24 \$/GJ (0.34 \$/therm) <sup>d</sup>	1.98 \$/GJ (0.21 \$/therm) <sup>d</sup>	27.68 \$/GJ (2.92 \$/therm) <sup>e</sup>
Traditional Fuel Emission Factor <sup>c</sup> @ 15 °C (59 °F) and 101.325 kPa (14.7 psi)	1926 gCO <sub>2</sub> /m <sup>3</sup> (0.120 lbCO <sub>2</sub> /ft <sup>3</sup> )	1888 gCO <sub>2</sub> /m <sup>3</sup> (0.118 lbCO <sub>2</sub> /ft <sup>3</sup> )	1887 gCO <sub>2</sub> /m <sup>3</sup> (0.118 lbCO <sub>2</sub> /ft <sup>3</sup> )	1928 gCO <sub>2</sub> /m <sup>3</sup> (0.12 lbCO <sub>2</sub> /ft <sup>3</sup> )	2.753 tCO <sub>2</sub> /m <sup>3</sup> (171.9 lbCO <sub>2</sub> /ft <sup>3</sup> )
Housing Stock <sup>f</sup>	282,355	846,405	564,230	287,775	3,210

<sup>a</sup>ASHRAE (2017)

<sup>b</sup>Rylan Urban (2020)

<sup>c</sup>Environment and Climate Change Canada (2019)

<sup>d</sup>Statistics Canada (2020a)

<sup>e</sup>Statistics Canada (2020b)

<sup>f</sup>Statistics Canada (2017)

analysis for the case study home. So, when the predicted area of each model was carried through subsequent calculations, its error was applied accordingly to provide an error range on the final energy consumption result.

- Ensure that effective training has been achieved by comparing the errors between the training and testing set. If training error is significantly greater than testing error, then the model was over-trained. Also, by checking how close Willmott's index approaches 1, it can be

found out if the model has good generalization and can make an accurate prediction on new data.

The generated files can predict each of the four output variables once a new set of input variables is known.

#### Heating load analysis

To assess the performance feasibility of ASHPs in existing homes across Canada, fundamental heat transfer principles were followed to quantify the energy demands of single-

**Table 4.** Resources consulted to find parameters needed for heat loss analysis.

Conduction		
Component	Surface Area	Thermal Transmittance
Above-grade Wall	SVR Model (Figure 1)	CSDDRD
Above-grade Roof	SVR Model (Figure 1)	CSDDRD
Below-grade Wall	SVR Model (Figure 1)	CSDDRD
Below-grade Floor	SVR Model (Figure 1)	CSDDRD
Window	CSDDRD	ASHRAE (2017)
Door	CSDDRD	CSDDRD
Convection		
Component	Flowrate	
Infiltration	CSDDRD	
Ventilation	ASHRAE (2016)	

**Table 5.** Basic specifications of heat pumps and furnaces to be used.

ASHP:	A	B	C	Furnace:	A	B <sup>a</sup>
Rated heating capacity @ 8 °C (46 °F)	12 kW (41 kBTU/h)	7 kW (24 kBTU/h)	16 kW (55 kBTU/h)	Fuel Type	Natural Gas	Light Fuel Oil
Outdoor operating temperature range (Lo/Hi)	−35 °C/15 °C (−31 °F/59 °F)	−20 °C/18 °C (−4 °F/64 °F)	−13 °C/30 °C (8.6 °F/86 °F)	Annual Fuel Utilization Efficiency (AFUE)	97%	95%
Coefficient of performance (COP) (Lo/Hi)	0.9/3.5	1.43/5.65	2.53/5.16	Heating Value of Fuel	0.0039 GJ/m <sup>3</sup> (1026 BTU/ft <sup>3</sup> )	39 GJ/m <sup>3</sup> (0.139 MBTU/gal)

<sup>a</sup>Furnace B only applies to Yellowknife.

detached houses in five cities: Vancouver, Edmonton, Toronto, Montreal, and Yellowknife. These cities were chosen because they represent populous regions with distinctly unique climate conditions. The heating load of each house in the database was evaluated under its corresponding outdoor conditions (99 % worst-case design temperature) and other descriptive parameters listed in Table 3. Furthermore, the analysis procedures for heating load evaluation were also taken from ASHRAE documentation referenced by the National Energy Code for Buildings (National Research Council of Canada 2017). The main forms of sensible heat loss considered in this study were conduction, infiltration, and ventilation; latent losses were not considered. As such, residential heat loss analysis was reduced to the set of governing parameters shown in Table 4. Conduction heat loss is a product of thermal transmittance of each exposed surface, its area, and the temperature difference across the boundary. Similarly, the convective loss is a function of flow rate, temperature difference between indoor and outdoor air. An indoor setpoint temperature was assumed to be 21 °C (70 °F) based on typical indoor conditions from ASHRAE (2017). The developed SVR models were used to predict the areas of the four main components of heat conduction through the envelope. To obtain the correct heating load analysis of the Canadian housing stock, data about fenestration, insulation values, and airtightness were taken from the CSDDRD. Since the thermal transmittance of windows

was not specified, a typical double-pane vinyl/wood frame window was assumed for all cases. ASHRAE Standard 62.2 (ASHRAE 2016) was consulted to approximate minimum ventilation flowrate depending on residence floor areas and the number of bedrooms. The resulting heat loss rates were integrated over a typical meteorological year; based on hourly temperature occurrence data from ASHRAE (2017) resourcesFormatting... please wait, which allowed us to visualize the total annual energy demand in addition to the average heat loss rate for homes in each city.

#### **Thermal balance and energy consumption**

Three commercially available heat pumps and two furnaces were examined in this feasibility study. These were selected based on a previous study, in which three models of heat pumps and three furnaces were compared and the best combination was found (Udovichenko and Zhong 2019). Table 5 shows a basic description of the two heating devices. First, the ASHP output capacity and residential heating load were compared as a function of outdoor temperatures, which was a means to identify the thermal balance point to switch from an ASHP to a furnace. Next, the total seasonal energy consumption of each heating system or combination was compared, which was computed based on the previously determined total annual heating energy demand using the hourly bin temperature data, mentioned earlier. Four

scenarios were assumed: a baseline case using only the furnace-alone (furnace A or B in Table 5) and three cases of a hybrid system composed of one ASHP with a furnace when needed. Since the natural gas furnace is not a common heating system in Yellowknife, an oil heating furnace (furnace B) was used as the traditional heating device in both the baseline and hybrid system cases for this city. In addition to the heat loss rate from each residence, the following parameters were calculated for each hour bin: heat loss from the residence, heat pump input and output, and supplemental heating amount (if any). Since the furnaces and heat pumps differ by energy type, no direct comparison was performed, but this analysis was used as an intermediate step to determine the final operating cost and GHG emissions results. However, a breakdown of system operation for the full year was determined, in which various stages of operation were added up based on the hourly count at each outdoor temperature occurring in the year. The stages of operation were split into the following cases: independent heat pump operation at part load with no supplemental heating (denoted as ASHP 'ON' and ASHP 'OFF' to account for cycling effects), full load operation with supplemental heating (denoted as ASHP 'ON' + Supplemental heating), and the case when the heat pump could not physically operate (denoted as ASHP 'OFF' + Supplemental heating).

### Model verification

A local Edmontonian home, which fits the description in Table A1, was used as a case study to validate the SVR predictions as well as the calculation of overall annual energy consumption. The inputs for the SVR models are shown in Table 6. Energy gas bills from the year of 2018 were analyzed to give the energy consumption of the natural gas furnace (80% AFUE) for space heating only. The indoor heating setpoint in this home was 18.5 °C (65.3 °F) in 2018, so a minor scaling adjustment had to be performed to stay consistent with the assumption of a 21 °C (70 °F) setpoint.

**Table 6.** Input variables of a case study in Edmonton.

Parameters	Value
Conditioned floor area	183.2 m <sup>2</sup> (1,970 ft <sup>2</sup> )
Perimeter of house footprint	41.4 m (136 ft)
Area of house footprint	107.0 m <sup>2</sup> (1,156 ft <sup>2</sup> )
House plan shape	Rectangular
Number of floors (above ground)	2
Number of bedrooms	3
Climatic zone	7
House vintage	1994

As mentioned in the SVR training, an uncertainty analysis was included to propagate the MAE associated with the SVR model predictions. In generating a comparable heating load, the insulation values and air change coefficients were necessary to be known, but they were not identified in the architectural drawings. To be consistent with the evaluation method for the homes in the database, the thermal transmittance and infiltration property were taken as the average value of year bin (1972–2003) and zone (7) from the CSDDRD.

### Economic and emissions analysis of heating systems

Once the total energy consumption of the heating systems was known, the economic and emissions analysis could be performed. The seasonal operating costs were calculated based on the utility costs associated with the two heating systems for each city. Similarly, GHG emissions associated with heating the residence were determined as a product of seasonal energy consumption and emission factors of the used energies. The utility costs for electricity, natural gas, and oil, as well as the emission factors, were found from websites of utility companies (Rylan Urban 2020), national statistics archives (Statistics Canada 2020b), and the national inventory report (Environment and Climate Change Canada 2019), respectively. The values shown in Table 3 were taken as an average over the last four years. This analysis does not include costs associated with utility transport and installation or maintenance of the equipment.

The GHG emissions results were expanded to a municipal level by considering the total housing stock (2017 census data from Statistics Canada) of each city. The total seasonal emissions for a city was estimated by the average of the emission results for each home in the database, multiplied by the total number of single-detached homes. This procedure assumes that the single-detached home database is statistically representative of the single-detached housing stock. In order to obtain a clear view about benefits of ASHP implementation, three scenarios were considered: A baseline, in which all homes are assumed to be using the traditional furnaces, either natural gas or fuel oil; a second scenario assumes half of the homes own an ASHP hybrid system; lastly, all homes in a city operate the hybrid system.

## Results and discussion

### SVR model results

The hyperparameter optimization of each model resulted in the optimal parameter values shown in Table 7. The

**Table 7.** Optimal parameters of SVR models.

	Basement Floor Area	Basement Wall Area	Ceiling Area	Gross Wall Area
Epsilon ( $\epsilon$ )	7.0288	4.2888	0.39952	0.46439
Box Constraint (C)	966.92	2.8495	26.584	0.063781
Kernel Function	linear	linear	linear	linear

**Table 8.** Performance evaluation results of four SVR models.

	Basement Floor Area		Basement Wall Area		Ceiling Area		Gross Wall Area	
	Train data	Test data	Train data	Test data	Train data	Test data	Train data	Test data
R <sup>2</sup>	0.87	0.86	0.77	0.71	0.81	0.87	0.96	0.95
MAE (m <sup>2</sup> )	9.28	9.49	9.16	9.56	8.57	8.68	8.16	8.78
RMSE (m <sup>2</sup> )	13.58	14.08	13.23	14.88	19.29	15.44	13.68	15.56
MAPE (%)	11.47	11.22	10.88	10.87	9.62	13.85	5.41	5.71
WI	0.82	0.95	0.76	0.94	0.85	0.96	0.92	0.98

**Table 9.** Model verification results (Case study).

	Actual	Predicted	% Error
Gross Wall Area, m <sup>2</sup> (ft <sup>2</sup> )	189.0 (2,034)	191.7 (2,063)	+1.4
Ceiling Area, m <sup>2</sup> (ft <sup>2</sup> )	107.0 (1,151)	103.9 (1,118)	-2.9
Basement Wall Area, m <sup>2</sup> (ft <sup>2</sup> )	98.0 (1,054)	92.7 (997)	-5.4
Basement Floor Area, m <sup>2</sup> (ft <sup>2</sup> )	107.0 (1,151)	91.0 (979)	-14.9

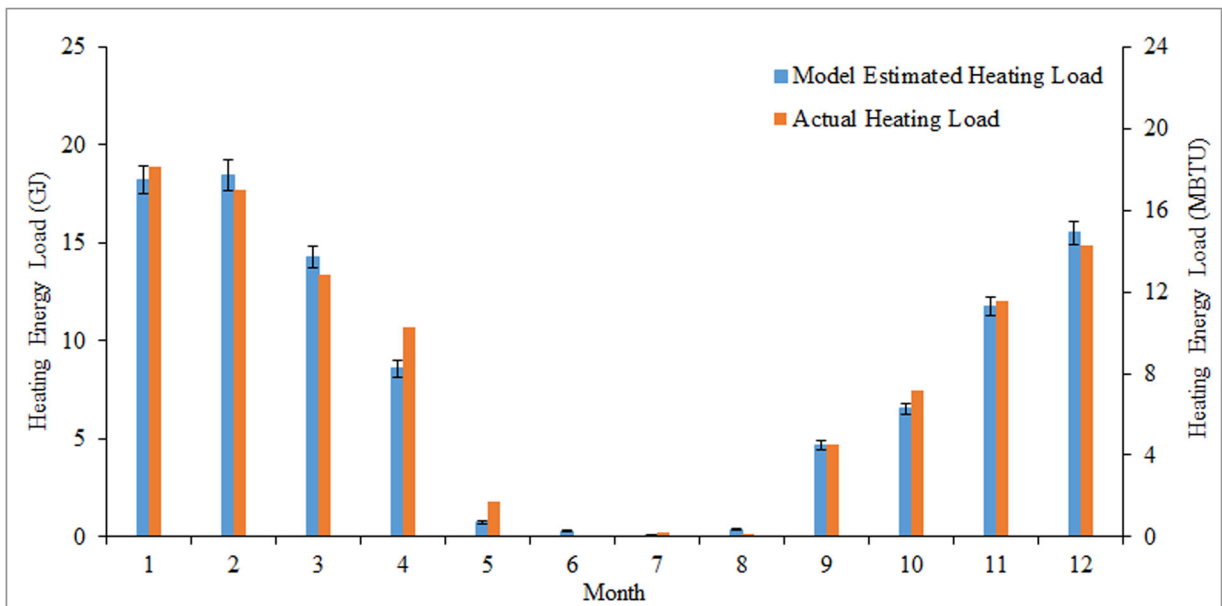


**Fig. 2.** Monthly space heating energy consumption of case study home.

programed optimization procedure tested different kernel functions and determined that the linear function was the most feasible for this type of data. Performance evaluation results for the four building-area models are displayed in Table 8. The gross wall area model was found to be the most accurate with a correlation coefficient of 0.96 and 0.95 for the train and test datasets, respectively, and with the lowest percentage errors. Meanwhile, the basement wall area showed moderate accuracy. However, all four models had MAPEs below 15% and the values of Wilmott’s index of agreement above 0.75, indicating good generalization capability. Comparing engineering drawing-based calculation areas with the predictions for the case study home, SVR models showed a good prediction capability in Table 9 for most outputs except for the basement floor area whose prediction error exceeded the MAPE of the developed model.

All other models achieved prediction errors below 10%. Overall, the gross above ground wall area model outperformed the other models based on R<sup>2</sup>, MAPE, WI, and prediction error.

**Model verification results**

The case study home was utilized to ensure that the procedures of energy consumption estimation following building-area prediction were valid in this study. The actual space heating load and the estimated consumption using ASHRAE procedures are compared in Figure 2. There was a good agreement between the actual and calculated energy consumption per month in 2018. The overall annual energy use of 102.0 GJ (97.5 MBTU) from the utility bill was comparable with 99.5 ± 1.5 GJ (94.3 ± 1.4 MBTU) from the energy

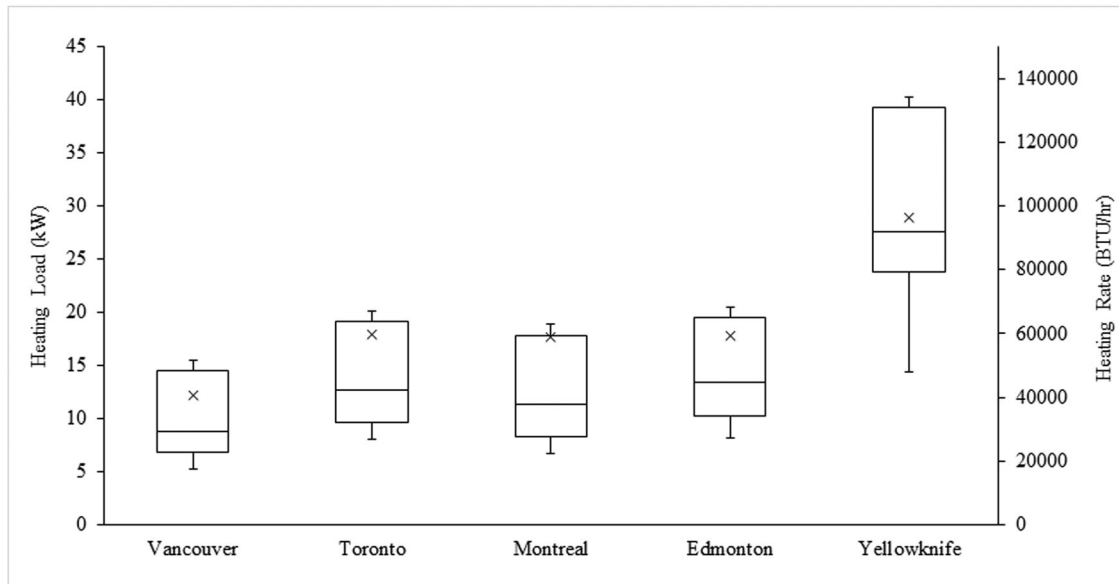


**Fig. 3.** Boxplots of design heating loads for five Canadian cities, where boxes represent the 25<sup>th</sup>, 50<sup>th</sup>, and 75<sup>th</sup> percentiles, the whiskers represent the 10<sup>th</sup> and 90<sup>th</sup> percentiles, x marks the mean value.

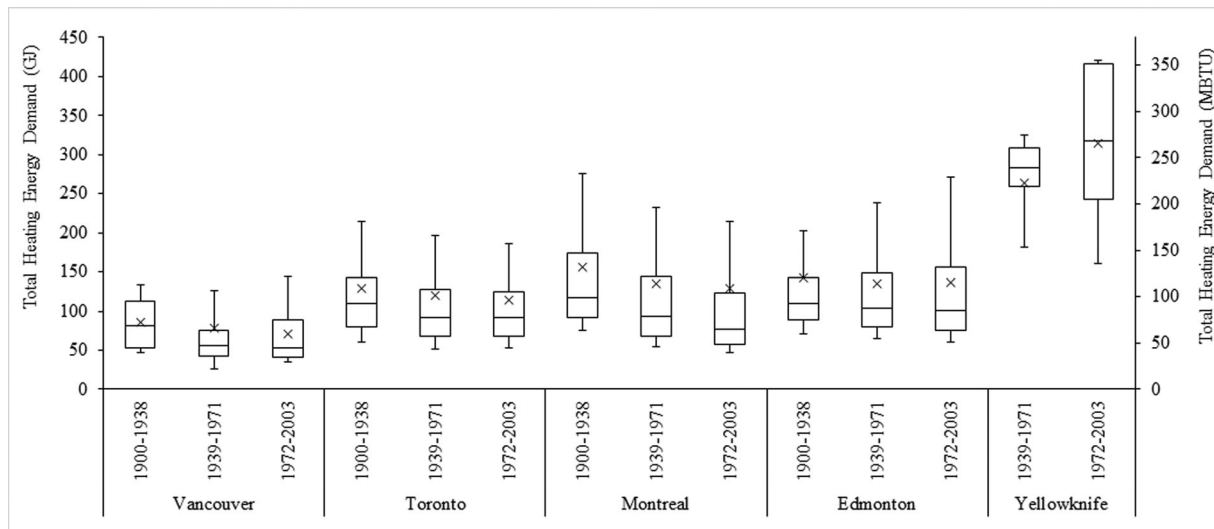


**Fig. 4.** Annual space heating energy consumption of a single-detached home using the best hybrid system in each city (natural gas furnace/ASHP-C in Vancouver, Toronto, Montreal, and Edmonton; oil furnace/ASHP-A in Yellowknife) based on vintage of home. No data was available for homes in Yellowknife in the '1900–1938' bin. Boxes represent the 25<sup>th</sup>, 50<sup>th</sup>, and 75<sup>th</sup> percentiles; the whiskers represent the 10<sup>th</sup> and 90<sup>th</sup> percentiles, x marks the mean value.

calculation, confirming that the house parameters predicted by the SVR models and the subsequent heat analysis were appropriate to be used in this study.

### Heating loads

As expected, the design heating loads for the cities worsen with harsher climate zones, as shown in Figure 3. Fundamentally, the colder cities experience higher design heating loads due to the lower design temperatures. 50% (25<sup>th</sup>–75<sup>th</sup> percentile) of the homes in Yellowknife have a design heating load in the

range of 23–39 kW (78480–133070 BTU/hr) due to the design temperature of  $-38.3^{\circ}\text{C}$  ( $-36.9^{\circ}\text{F}$ ). Meanwhile, the same fraction of homes in Vancouver would experience a heat loss rate of 7–14 kW (23880–47770 BTU/hr) at a temperature of  $-3.4^{\circ}\text{C}$  ( $25.9^{\circ}\text{F}$ ). Surprisingly, the design temperature decrease between Toronto at  $-13.7^{\circ}\text{C}$  ( $7.3^{\circ}\text{F}$ ), Montreal at  $-19.2^{\circ}\text{C}$  ( $-2.6^{\circ}\text{F}$ ), and Edmonton with  $-25.8^{\circ}\text{C}$  ( $-14.4^{\circ}\text{F}$ ) results in fairly constant heating loads for the 25<sup>th</sup>–75<sup>th</sup> percentiles of 10–19 kW (34120–64830 BTU/hr), 8–18 kW (27297–61418 BTU/hr), 10–19 kW (34121–64830 BTU/hr), respectively. Since thermal resistances (Figure A2) for different

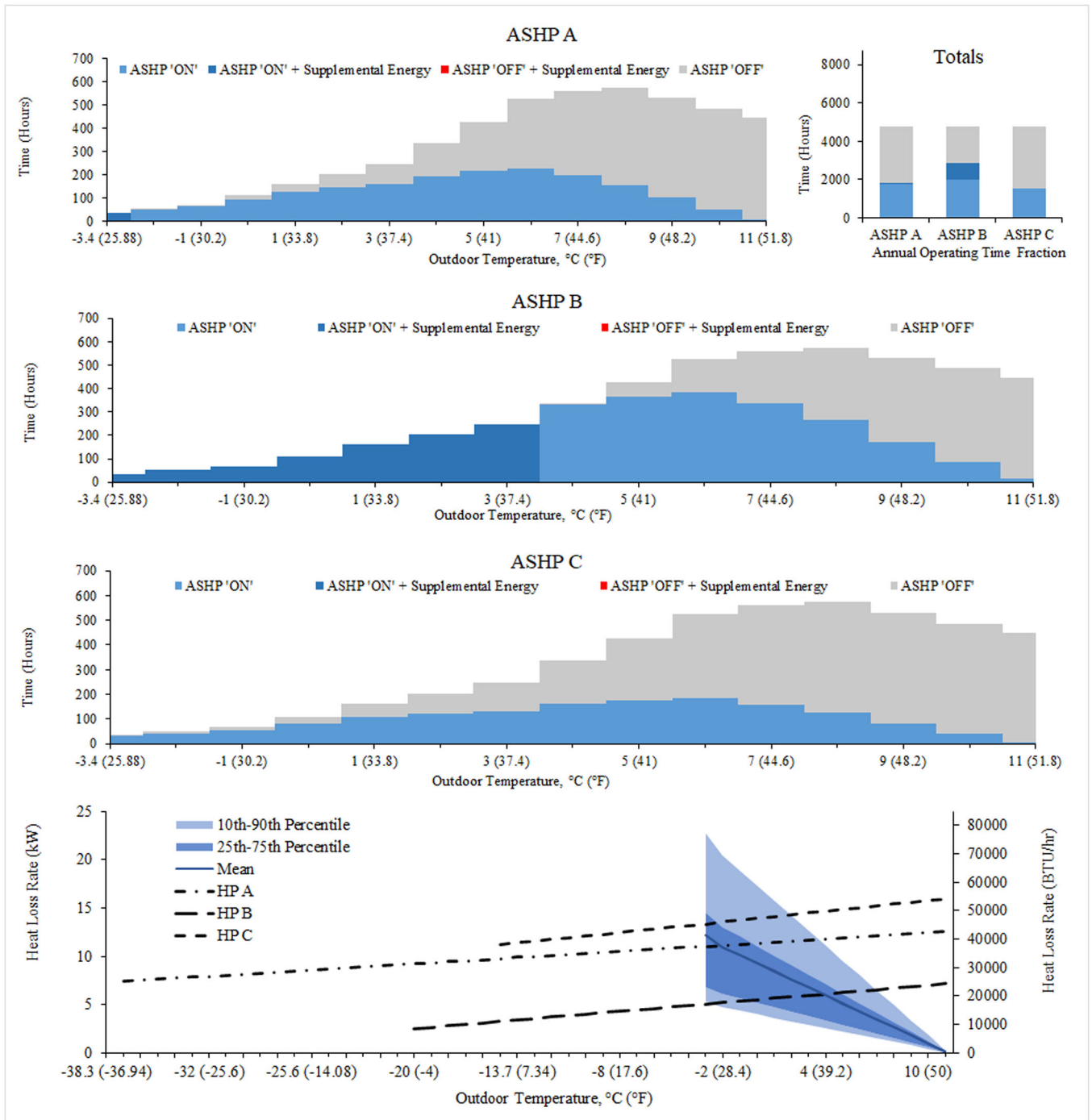


**Fig. 5.** Heating load and ASHP capacity as a function of outdoor temperature for Vancouver (lower). Annual heating temperature bins for all ASHPs (centre), and operating time fraction (upper right) of the three ASHPs for an average home.

components across the zones are relatively constant, these results could be attributed to the exposed surface areas. For example, Vancouver’s (zone 4) mild design temperature is countered by its larger exposure areas, which results in the heating load stated above. Table 1 shows a decreasing trend of house sizes from Vancouver (zone 4), Toronto (zone 5), Montreal (zone 6) to Edmonton (zone 7), which is the reason for the similar heating loads in these cities. In Yellowknife (zone 8), the extreme outdoor conditions coupled with a

noticeable reduction in below-ground component insulation values result in much harsher design loads. Even though the housing component areas are lower for Yellowknife, this change is not enough to counter the magnitude of heat loss occurring.

Figure 4 presents a set of cumulative results deduced from the heating loads, on a vintage basis over the last century. The total annual energy demand in each city was plotted based on year bin clusters. In general, the magnitude of energy consumption in each city closely resembles the trends

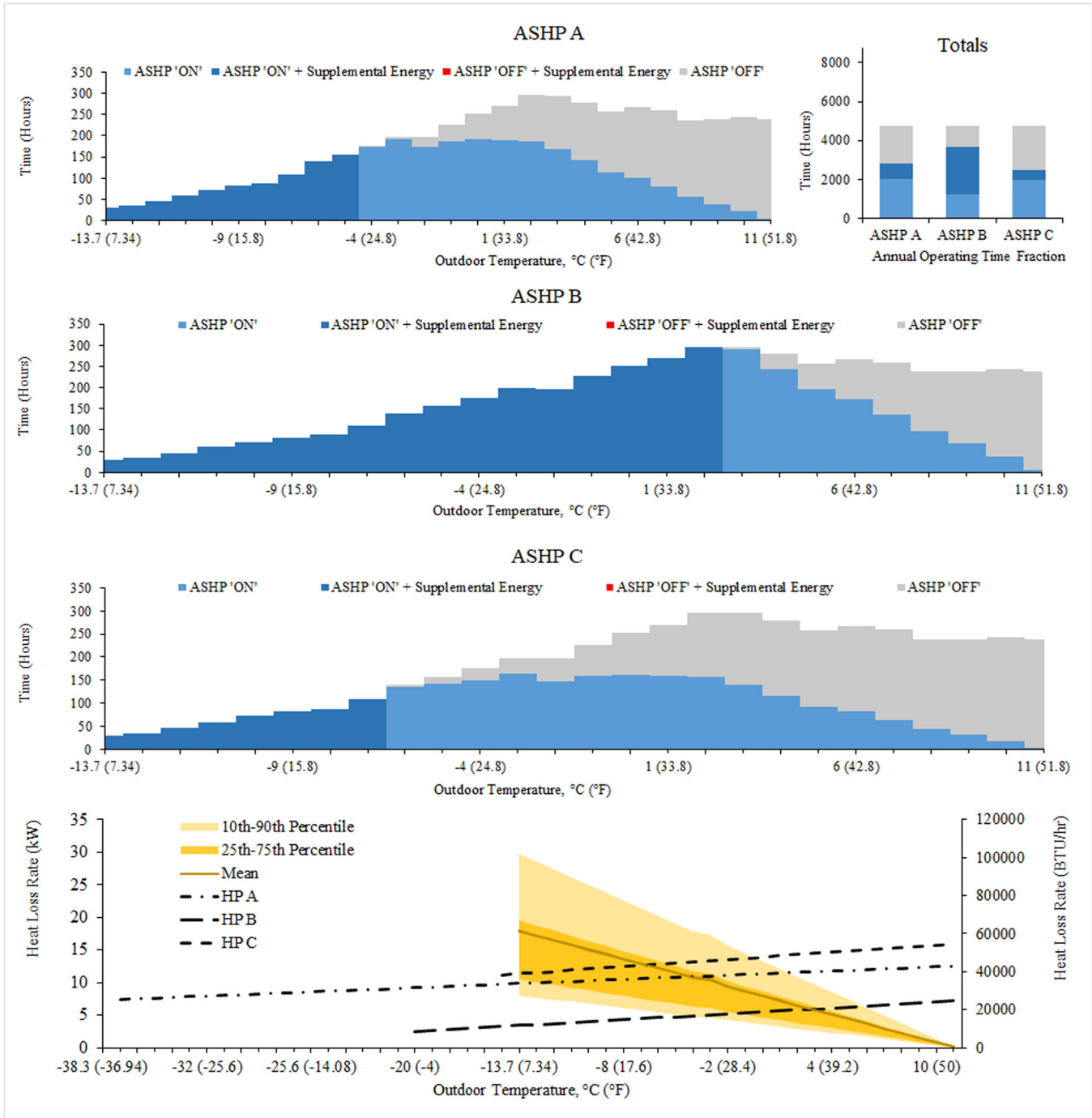


**Fig. 6.** Heating load and ASHP capacity as a function of outdoor temperature for Toronto (lower). Annual heating temperature bins for all ASHPs (centre), and operating time fraction (upper right) of the three ASHPs for an average home.

of design-case heat loss in Figure 3. Yet, now there is evidence of older homes having higher energy needs as compared with more modern homes. In Vancouver, compared with homes built between 1900 and 1938, mid-century and late-century homes consume 91 % and 82% as much energy, which showcases noticeable improvements in housing quality toward the end of the century. Similarly, homes built in Toronto between 1939–1971 and 1972–2003 have achieved

energy consumptions of 92 % and 88 % as large as homes built at the start of the century, respectively. Montreal and Edmonton have seen diminishing results, with mid- and late-century homes achieving energy consumptions of 87 % and 83 % in Montreal, and 95 % and 96 % in Edmonton as high as homes built between 1900 and 1938 in those locations. Since the reduced dataset lacked early century homes for Yellowknife, less can be analyzed about this city. Newer

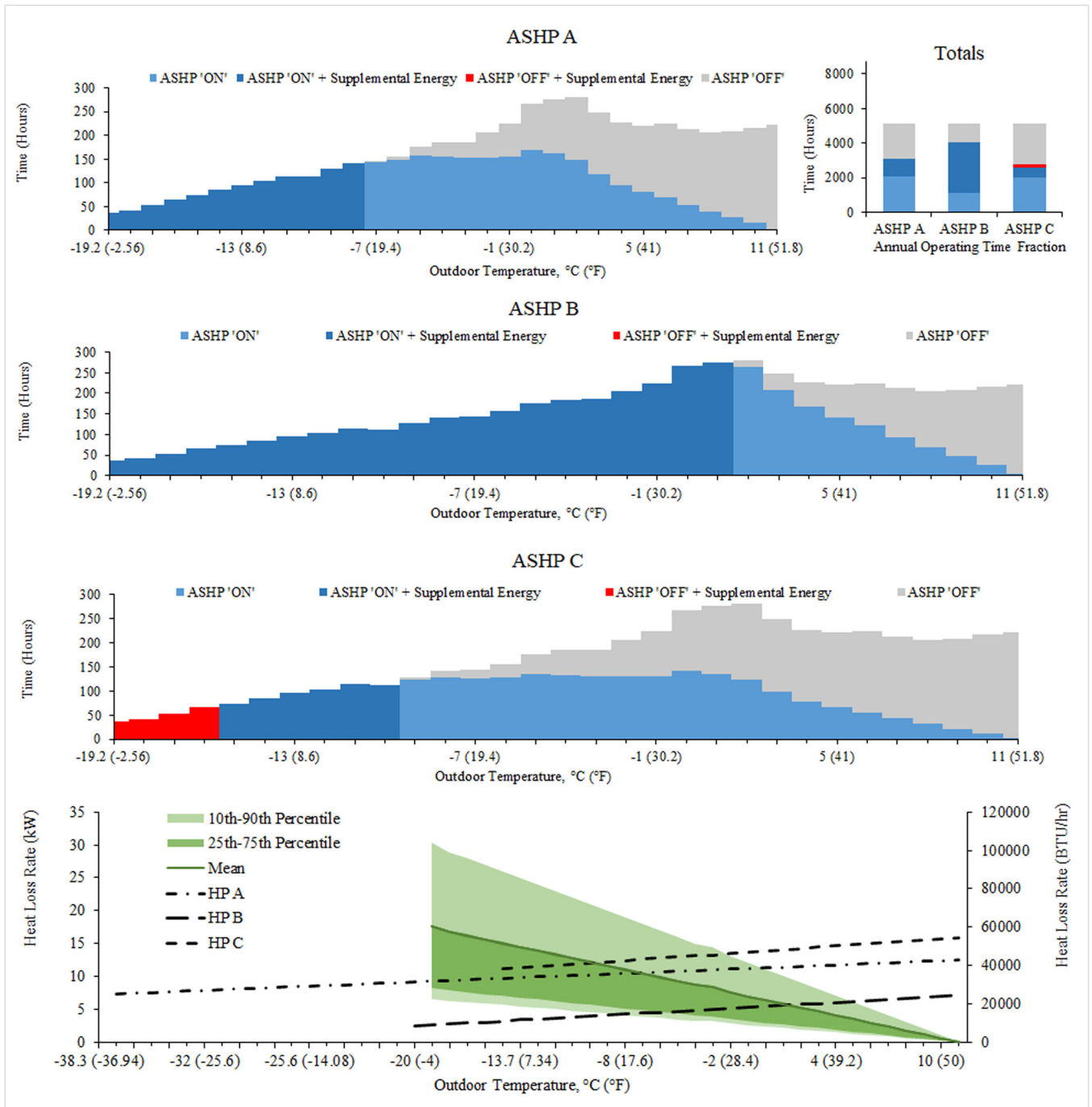


**Fig. 7.** Heating load and ASHP capacity as a function of outdoor temperature for Montreal (lower). Annual heating temperature bins for all ASHPs (centre), and operating time fraction (upper right) of the three ASHPs for an average home.

homes appear to have higher energy consumptions (19 % increase) than older homes. Overall, this is evidence of noticeable innovation with regards to housing technologies and practices having taken place over the last century. However, a more drastic reduction was expected.

**Thermal balance and energy consumption**

Figures 5–9 present the heating loads of each city as a function of outdoor temperature, as well as the temperature-dependent heat

capacity of three ASHPs. The intersection of the average heating load curve and the capacity curve signifies the average thermal balance point of the ASHP operating in that location. The temperature bin plots are meant to breakdown the various stages of heating system operation that would occur for an average home, heated with hybrid systems consisting of each of the heat pumps and the corresponding furnace for each city. This information is also summarized as a total for each system on an annual basis.

For Vancouver, the mild conditions allow all three ASHPs to operate at all the outdoor temperatures. This means that, in

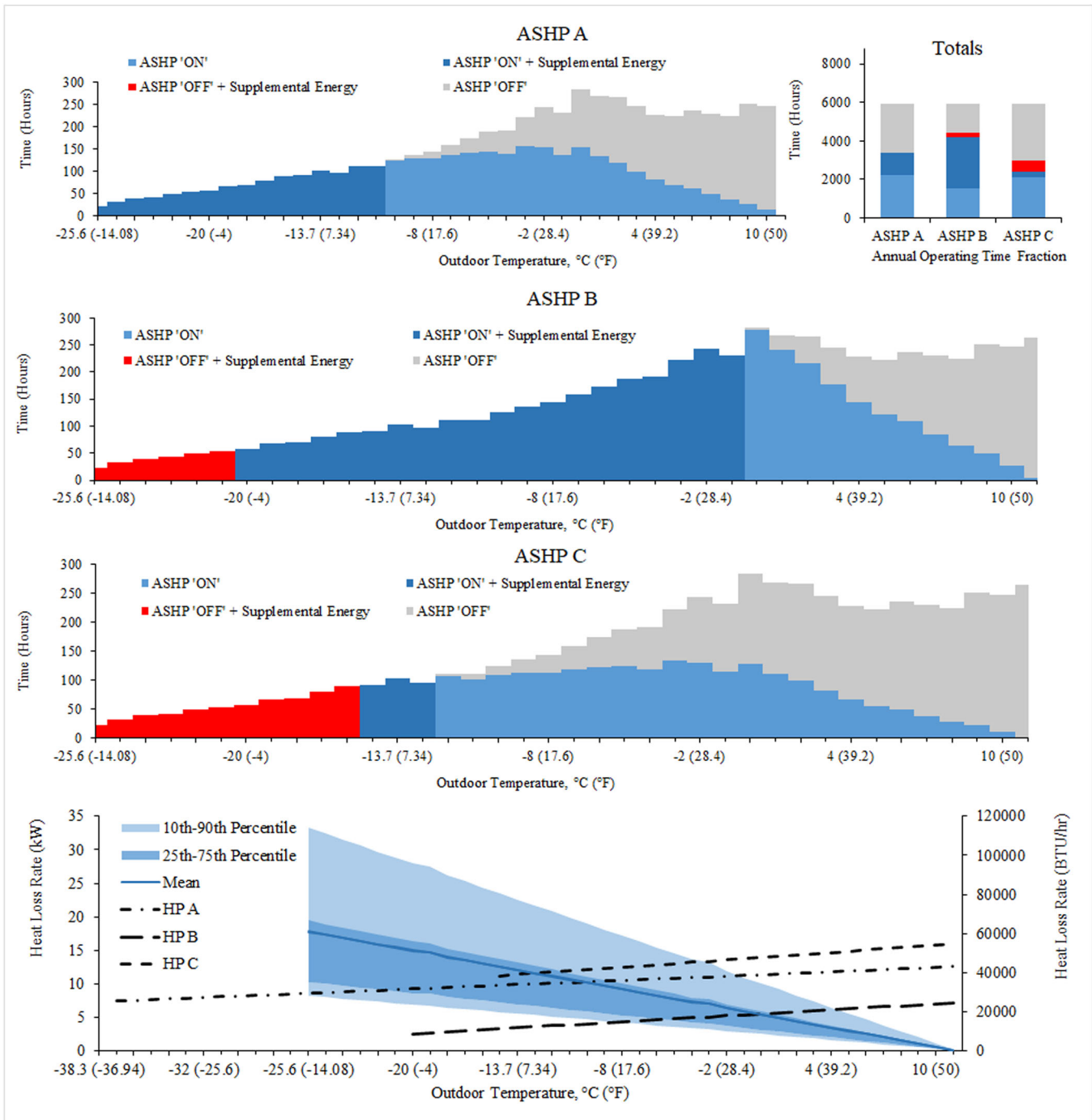


**Fig. 8.** Heating load and ASHP capacity as a function of outdoor temperature for Edmonton (lower). Annual heating temperature bins for all ASHPs (centre), and operating time fraction (upper right) of the three ASHPs for an average home.

general, all three models can provide heat without operational limitations. However, the heat capacity is limited for all three models, and supplemental heating is required for all homes except the bottom ~50 %, whose energy demands can be fully covered by A- and C- ASHPs (Figure 5). Furthermore, an average home in Vancouver could be heated only with ASHP C; at part load and without supplemental heating, for the entirety of the 4757-hour heating season, while only operating for 1500 hours (22 % of the time). In contrast, ASHP B would

have to be ‘on’ for 2830 hours in the winter, including 872 hours (13 % of the time) that would require supplemental energy. Overall, this suggests that in the warmest city in Canada, most of currently available ASHPs possess the heat capacity to satisfy the heating requirements of ~50 % of the homes at an outdoor temperature of  $-3.4\text{ }^{\circ}\text{C}$  ( $25.9\text{ }^{\circ}\text{F}$ ), with minimal or no supplemental heat.

The results are noticeably worse for Toronto (Figure 6); all the models can function, but supplemental energy is

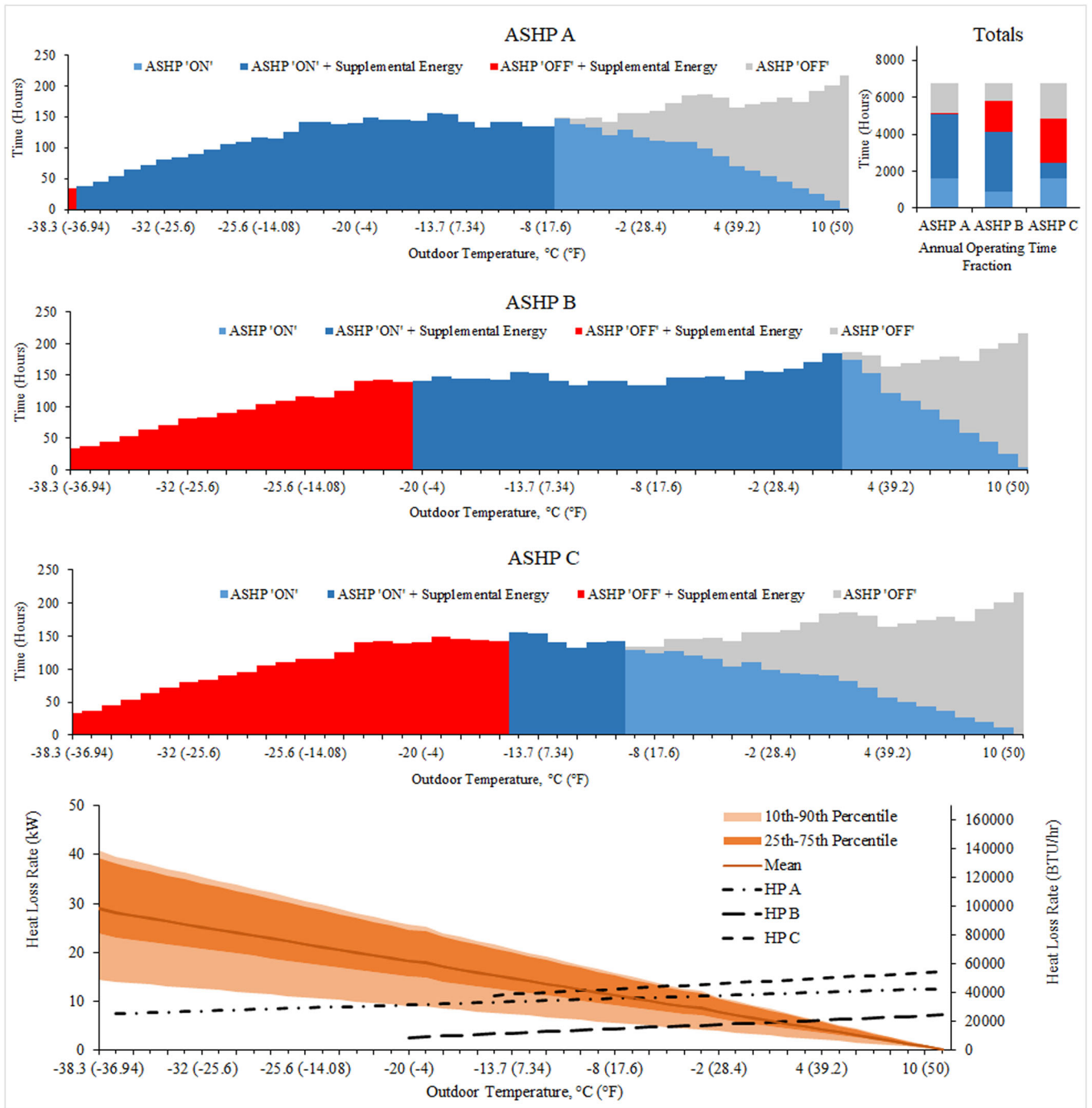


**Fig. 9.** Heating load and ASHP capacity as a function of outdoor temperature for Yellowknife (lower). Annual heating temperature bins for all ASHPs (centre), and operating time fraction (upper right) of the three ASHPs for an average home.

required for all of them. Only the bottom ~25 % of homes with the lowest heating loads can be satisfied with the best heat pumps (ASHPs A & C) operating independently of auxiliary systems. If ASHP B were to be used, that fraction would go down to far below 10 % of homes. ASHP operating time during the 4750-hour heating season would range between 2488 hours (37 %) in total including 520 hours (8 %) of supplemental heating for ASHP C and 3683 hours (55 %) in total with 2433 hours (36 %) of supplemental heating

for ASHP B. It is evident that these operating time variations are what create a large impact on the final energy consumption, and therefore, heavily impact cost and emissions savings.

As the locations get colder, the limitations of the heat pumps become more prevalent. Montreal and Edmonton's conditions are too harsh for some ASHP models to function year-round (Figures 7 and 8). However, the insulation and surface area trends, discussed previously, result in these two

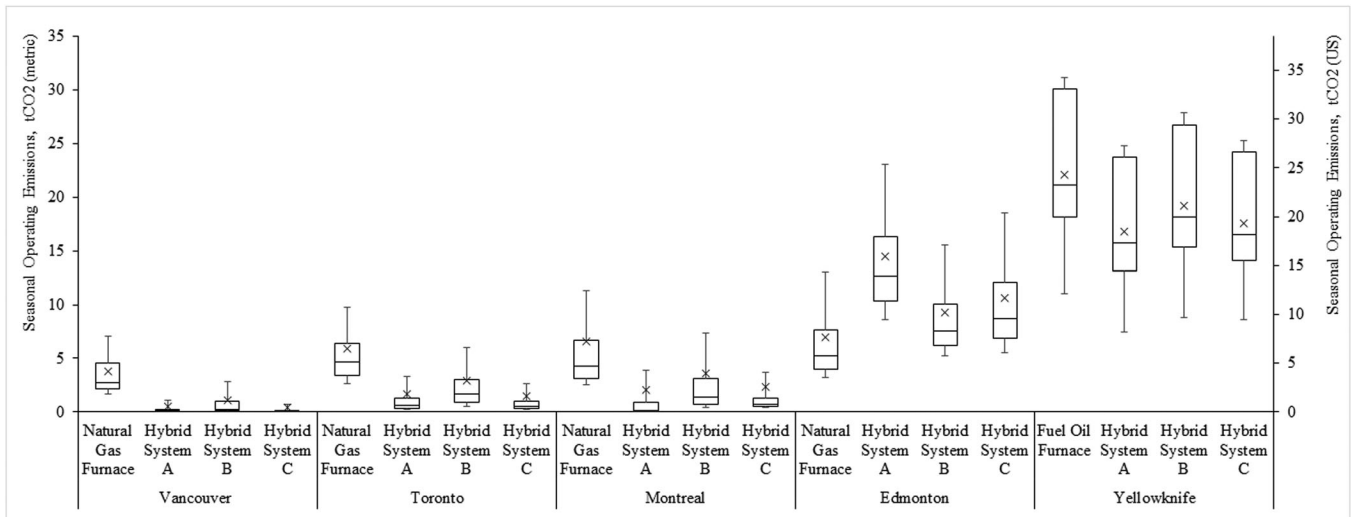


**Fig. 10.** The seasonal CO<sub>2</sub> emissions for a single-detached home in each city using the four systems. Boxes represent the 25<sup>th</sup>, 50<sup>th</sup>, and 75<sup>th</sup> percentiles; the whiskers represent the 10<sup>th</sup> and 90<sup>th</sup> percentiles, x marks the mean value.

locations having operating time fraction comparable to that of Toronto. A high capacity model (ASHP C) would have to operate independently for 1980 hours (29 %), in dual-device operation for an additional 584 hours (9 %), and would be physically incapable of operating for 198 hours (3 %), which would have to be entirely supported by the furnace. On the contrary, ASHPs A and B would have no physical limitations, but would have to operate at full-load for much longer; 2046 hours (30 %) independently plus 1052 hours (16 %) with supplemental energy for ASHP A, and 1146 hours (17 %) independently and 2870 hours (42 %) with supplemental energy for ASHP B. For Edmonton, ASHP B's 1515 hours (22 %) in part load operation, 2691 hours (40 %) with auxiliary heating and 240 hours (4 %) in shut-off mode, showcases the obvious weakness of a low-capacity model with an intermediate operating temperature range. In total, the operating times of the three units (A, B, C) are 3098, 4016, and 2561 hours in Montreal, and 3358, 4206, and 2397 hours in Edmonton, which is consistent with the total heating hours of 5137 and 5897 for an average residence in the two cities, respectively. Furthermore, one advantage of ASHP A's low operating temperatures, is that it is the only model that can support a fraction of homes with no need for supplemental systems, even though that fraction is ~25 % in Montreal, and ~10 % in Edmonton.

Unsurprisingly, all three systems will struggle in Yellowknife, so there are no homes that can run solely on electric heat pump heating during the 6750-hour heating season (Figure 9). Supplemental energy operation would have to occur for 2371 hours (35 %) for ASHP C to 33 hours (0.5 %) for ASHP A. In this case, independent heating time becomes irrelevant and focus shifts to finding the ASHP model that can achieve greater operating times with auxiliary energy. Even though ASHP-C has a lower switch temperature of  $-5.5^{\circ}\text{C}$  ( $22.1^{\circ}\text{F}$ ) than ASHP-A's  $-2.3^{\circ}\text{C}$  ( $27.9^{\circ}\text{F}$ ), the latter has a much greater presence in the heating season due to its ability to stay active at extremely cold temperatures. Therefore, ASHP-A can supply low quality heat for a

greater portion of the heating season than its counterparts, even if only to satisfy a part of the required load. However, the quality of heat provided by ASHP-A at most of these temperatures can be minimal, as compared with the overall greater output from ASHP-C, as can be deduced from inspection of the heat capacity outputs in the bottom of Figure 8. This dynamic between the heat pump models can result in vastly different cost and emissions implications depending on various external factors, such as energy availability, cost, and emissions factors.

Figure A3 shows the ranges of annual heating energy required for a home in each city using the four heating systems. Furthermore, the hybrid system that shows the lowest energy consumption (natural gas furnace/ASHP-C in Vancouver, Toronto, Montreal, and Edmonton; oil furnace/ASHP-A in Yellowknife) can be broken down into its components, as shown in Figure A4. These plots can be used to show the overall mixed source energy supply to the system from the end user perspective. However, the since these are a combination of primary and secondary energy sources, conclusions cannot be drawn regarding energy savings. Instead, these are directly linked to the economic and emissions results computed later.

### *Economic and emissions feasibility*

Annual operating emissions and costs are shown in Figures 10 and 11. Operating the hybrid system is expected to provide a reduction in seasonal emissions in the homes of Vancouver of 71–89 %, with hybrid system C providing the greatest benefit. Similarly, homes in Toronto could reduce their emissions by 50 % if ASHP B is used, 71 % if ASHP A is used, and by 76 % if ASHP C is used. The superiority of heat pumps A and C, which was partially evident during thermal balance and operating time analysis, is further reinforced by the results of Montreal. The average home in this city could reduce their operating emissions by at least 45% with hybrid system B, and at most by 69 % with hybrid

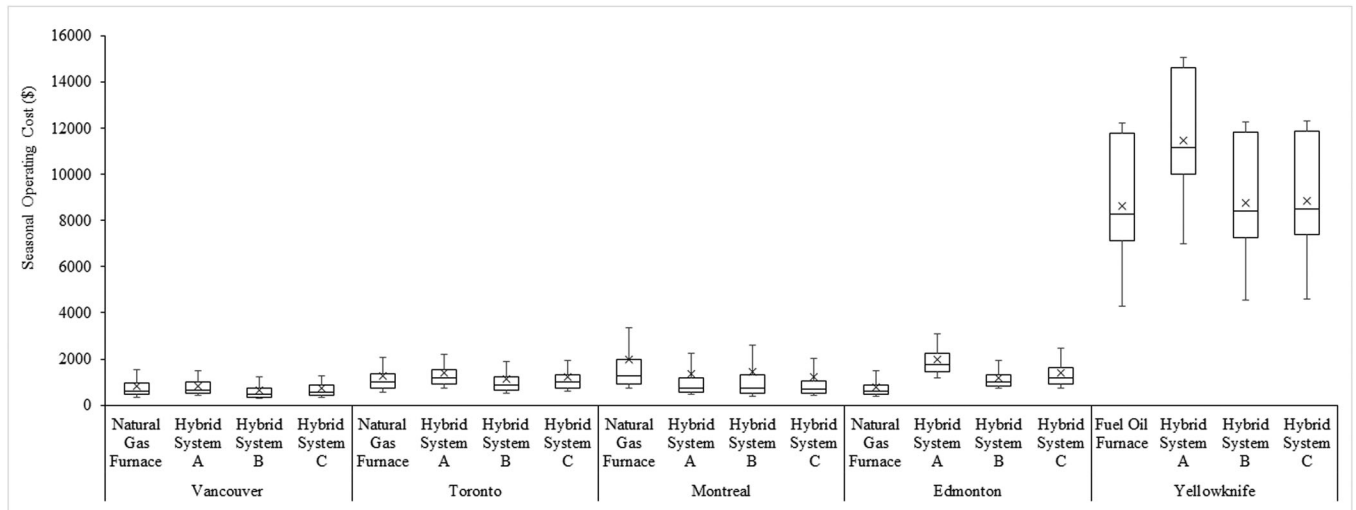


**Fig. 11.** The seasonal operating cost for a single-detached home in each city using the four systems. Boxes represent the 25<sup>th</sup>, 50<sup>th</sup>, and 75<sup>th</sup> percentiles; the whiskers represent the 10<sup>th</sup> and 90<sup>th</sup> percentiles, x marks the mean value.

system A. This effect is associated with the generation mix of electricity supplied to these locations. For example, 99% and 90% of the electricity produced in Quebec and British Columbia, respectively, comes from renewable sources such as hydro, tidal, solar, and wind (National Energy Board 2020). In Ontario, that number is only 33%, but an additional 60% comes from nuclear steam turbine generation (National Energy Board 2020). In large contrast, Edmontonian homes would experience an emissions increase of 25 % (hybrid system B), 35% (hybrid system C), and 52 % (hybrid system A). This is due to the fact that 93% of electricity in Alberta is generated by the combustion of fossil fuels (National Energy Board 2020); an issue that is currently being tackled in the province's energy sector (Weis, Thibault, and Miller 2016). In the case of Yellowknife, 33 % of electricity is generated renewably (National Energy Board 2020), so the hybrid system would bring about emissions reduction of up to 24 % if hybrid system A is used (20 % for ASHP C and 13 % for ASHP B), but the magnitude of emissions far exceeds an average home in any other city due to the heavy reliance on heating oil. This result also reinforces the fact that a lower capacity ASHP A that can operate for a greater portion of the season is more beneficial than a higher capacity ASHP C, which far more limited in the operating temperature range.

With regard to average seasonal operating costs, the results are once again region-dependent and do not exactly parallel the results presented directly above. Operating the hybrid system would mean cost reductions of 10% or 20% if hybrid systems C and B are used, respectively. However, usage of ASHP A in conjunction with the traditional furnace in a typical Vancouver home would increase annual spending by 4%. This can be attributed to its having the lowest efficiency as denoted by its coefficient of performance (COP) in Table 5. This trend in operating costs extends to Toronto, where reduction of 3 % and 8 % can be achieved with ASHPs C and B, respectively, but ASHP A generates an increase of 13 % in annual operating costs. This suggests

that there is currently no single system that can objectively outperform the rest by both metrics. While hybrid system C is certainly a strong choice in these locations, a decision must be made based on what the consumer values. The most positive results occur in Montreal, where electricity price is by far the lowest amongst the five cities (Hydro-Québec 2020), which leads to a reduction in costs between 27 % (ASHP B), 31 % (ASHP A), and 37 % (ASHP C). In contrast, the low cost of natural gas in Alberta signifies that the average operational cost could increase by 33–60 % in Edmonton if the average home installs hybrid systems B or C, respectively. Likewise, expenditures would increase in Yellowknife due to high electricity costs by as much as 25 % for hybrid system A. However, operating hybrid systems B and C would only increase by 1 and 2 %, respectively. As such, it is concluded that both emissions and cost reduction from the ASHP technology favor Vancouver, Toronto and Montreal. However, no single system can achieve the greatest reductions in operating GHG emissions and annual costs simultaneously.

Although the results are not entirely favorable, the implications from emissions results are very positive, especially since the nation is aiming to reduce its emissions through various goals. Mainly, the Paris Agreement pledges to reduce national emissions by 30 % by 2030 compared to 2005 levels (Mascher 2018). Thus, a municipal-level analysis could be of use for visualizing potential emissions-reduction strategies. Figure 12 presents a few potential scenarios for emissions reduction on a greater scale. If every home in Vancouver were to switch to using a hybrid ASHP C-furnace system, overall annual heating emissions would reduce by 8 %. Similarly, in Montreal by 22 % with hybrid system A. With Toronto's massive population and housing stock, making the switch to all hybrid with ASHP-C systems in this city would result in the greatest overall reduction in residential heating emissions of these five communities of 32 %. By contrast, Edmonton's case would increase the CO<sub>2</sub> release of the cities by 5 % even if the least polluting hybrid

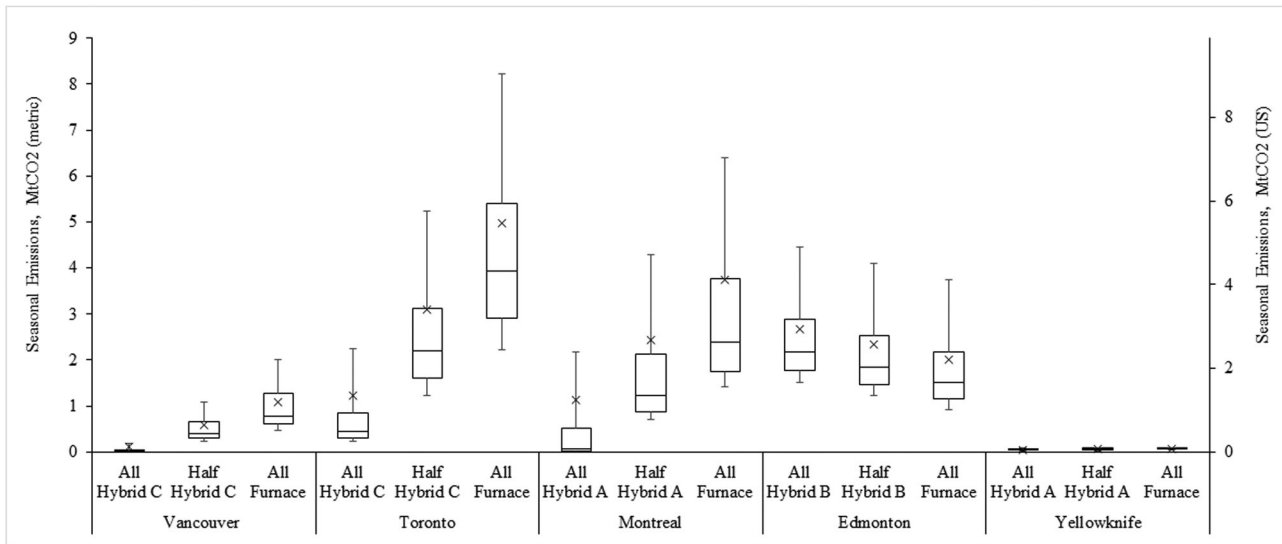


**Fig. 12.** Municipal-scale GHG emissions results for all single-detached homes in each city at three heat operating scenarios. Boxes represent the 25<sup>th</sup>, 50<sup>th</sup>, and 75<sup>th</sup> percentiles; the whiskers represent the 10<sup>th</sup> and 90<sup>th</sup> percentiles, x marks the mean value.

system (B) was used in an all-hybrid scenario. Yellowknife's extreme emissions do not have such a major impact due to its relatively low population community (emission decrease of only 0.14 % for the combination of residential communities).

### Limitations

This study was simplified and limited in several of the following ways. Firstly, the target and input selection in this study heavily relied on the data provided from the database, so it is possible that replicating the procedure on different sets of housing data could result in different variables with better-correlating relationships. Furthermore, it is critical to note that although the original data regarding the four main components were available for use in the techno-economic analysis, prediction results from the SVR modeling were used instead. The reasoning behind this decision was to showcase the process of how the SVR predictions can be acquired and then utilized in housing energy analysis. The goal is to replicate this procedure on other datasets for different styles of homes, such as double/rowhouses, in other countries to model the necessary parameters completely. Given that the four targets tested here gave positive results, the SVR models could be expanded to other housing parameters, primarily the ones which were not feasible in this study, such as infiltration coefficients and fenestration areas. Regarding the techno-economic analysis procedure, additional steps could be taken to involve a greater level of detail in the analysis. For example, the heating load calculations may be modified to include other heat transfer effects, such as humidity, wind speed, and hourly solar irradiance. Similarly, the economic analysis in this study ignores the costs of energy transmission, as well as equipment installation and maintenance costs. Furthermore, ASHP technology can be used for cooling purposes, leading to costs and GHG

emissions as well, which is beyond the scope of this study given the considerable heating demand in Canada.

### Conclusion

Given that more than half of Canada's electricity production comes from renewable sources (Environment and Climate Change Canada 2016), utilizing electric heating where possible would greatly aid in achieving Canada's long-term emissions goals. This study analyzed the effect of utilizing electric ASHPs for residential heating in several Canadian cities. Prior to the feasibility analysis, SVR was applied to a Canadian housing database to generate predictive models for architectural exposure areas that were used to estimate heating energy consumption. This validated method showed reliability and consistency in analyzing large datasets. Heating load, economic and emissions analysis showed that ASHP technology would be beneficial to bring about energy source changes in the residential sector: increased use of electricity and lowered the consumption of traditional heating fuels. Moreover, the ASHP system would introduce seasonal cost reduction in Vancouver, Toronto, and Montreal. The heavily renewable generation mix and moderate utility costs, coupled with milder climates, make these locations suitable for the ASHP system and can benefit from cost and emissions reduction for space heating. Yellowknife could benefit from this system only through GHG emissions reduction, as operating costs would increase moderately. Meanwhile, currently available ASHP technology is temporarily unfeasible for use by every measurable margin in Edmonton due to a lack of renewable electricity. However, some provincial governments are actively developing renewable technology to boost green electricity, such as the new solar farms scheduled for development in southern Alberta (Government of Alberta 2020), which will facilitate ASHP technology implementation in Canada.

## Funding

This work was supported by the Natural Sciences and Engineering Research Council of Canada under the Discovery Grant [RGPIN-2018-05130].

## References

- Alshehri, F., S. Beck, D. Ingham, L. Ma, and M. Pourkashanian. 2019. Techno-economic analysis of ground and air source heat pumps in hot dry climates. *Journal of Building Engineering* 26: 100825. <https://doi.org/10.1016/j.jobte.2019.100825>. <http://www.sciencedirect.com/science/article/pii/S2352710219302001>.
- Amirirad, A., R. Kumar, and A. S. Fung. 2018. Performance characterization of an indoor air source heat pump water heater for residential applications in Canada. *International Journal of Energy Research* 42 (3):1316–27. doi:<https://doi.org/10.1002/er.3932>
- ASHRAE. 2016. *Ventilation and acceptable indoor air quality in residential buildings*. Atlanta, GA: ASHRAE.
- ASHRAE. 2017. *2017 ASHRAE handbook*. Atlanta, GA: ASHRAE.
- Bertsch, S. S., and E. A. Groll. 2008. Two-stage air-source heat pump for residential heating and cooling applications in northern U.S. climates. *International Journal of Refrigeration* 31: 1282–92. <https://doi.org/10.1016/j.ijrefrig.2008.01.006>. <http://www.sciencedirect.com/science/article/pii/S0140700708000273>.
- Chen, Y., P. Xu, Y. Chu, W. Li, Y. Wu, L. Ni, Y. Bao, and K. Wang. 2017. Short-term electrical load forecasting using the Support Vector Regression (SVR) model to calculate the demand response baseline for office buildings. *Applied Energy* 195: 659–70. <https://doi.org/10.1016/j.apenergy.2017.03.034>. <http://www.sciencedirect.com/science/article/pii/S0306261917302581>.
- Demirezen, G., N. Ekrami, and A. S. Fung. 2019. Monitoring and evaluation of Nearly-Zero Energy House (NZEH) with hybrid HVAC for cold climate – Canada. *IOP Conference Series: Materials Science and Engineering* 609: 62001. <http://dx.doi.org/10.1088/1757-899X/609/6/062001>
- Di Placido, A. M., K. D. Pressnail, and M. F. Touchie. 2014. Exceeding the Ontario building code for low-rise residential buildings: Economic and environmental implications. *Building and Environment* 77: 40–9. <https://doi.org/10.1016/j.buildenv.2014.03.015>. <http://www.sciencedirect.com/science/article/pii/S0360132314000754>.
- Environment and Climate Change Canada. 2016. Canada's mid-century long-term low-greenhouse gas development strategy. [http://unfccc.int/files/focus/long-term\\_strategies/application/pdf/canadas\\_mid-century\\_long-term\\_strategy.pdf](http://unfccc.int/files/focus/long-term_strategies/application/pdf/canadas_mid-century_long-term_strategy.pdf).
- Environment and Climate Change Canada. 2019. National Inventory Report 1990–2017: Greenhouse gas sources and sinks in Canada. Accessed February 13, 2020. [http://publications.gc.ca/collections/collection\\_2019/eccc/En81-4-2017-2-eng.pdf](http://publications.gc.ca/collections/collection_2019/eccc/En81-4-2017-2-eng.pdf).
- Goudarzi, S., M. Hossein Anisi, N. Kama, F. Doctor, S. A. Soleymani, and A. K. Sangaiah. 2019. Predictive modelling of building energy consumption based on a hybrid nature-inspired optimization algorithm. *Energy and Buildings* 196: 83–93. <https://doi.org/10.1016/j.enbuild.2019.05.031>. <http://www.sciencedirect.com/science/article/pii/S0378778819304177>.
- Government of Alberta. 2020. Alberta major projects. Accessed February 19, 2020. <https://majorprojects.alberta.ca>.
- Grossi, I., M. Dongellini, A. Piazzini, and G. L. Morini. 2018. Dynamic modelling and energy performance analysis of an innovative dual-source heat pump system. *Applied Thermal Engineering* 142: 745–59. <https://doi.org/10.1016/j.applthermaleng.2018.07.022>. <http://www.sciencedirect.com/science/article/pii/S1359431118309128>.
- Guoyuan, M., C. Qinhu, and J. Yi. 2003. Experimental investigation of air-source heat pump for cold regions. *International Journal of Refrigeration* 26: 12–8. [https://doi.org/10.1016/S0140-7007\(02\)00083-X](https://doi.org/10.1016/S0140-7007(02)00083-X). <http://www.sciencedirect.com/science/article/pii/S014070070200083X>.
- Huang, M. J., and N. J. Hewitt. 2013. The experimental analysis of the effect of ambient factors on the defrosting of economised vapour injection compressor air source heat pump in marine climates. *International Journal of Refrigeration* 36: 820–7. <https://doi.org/10.1016/j.ijrefrig.2012.10.018>. <http://www.sciencedirect.com/science/article/pii/S0140700712002782>.
- Hydro-Québec. 2020. Comparison of electricity prices. <http://www.hydroquebec.com/residential/customer-space/rates/comparison-electricity-prices.html>.
- Jhee, S., K.-S. Lee, and W.-S. Kim. 2002. Effect of surface treatments on the frosting/defrosting behavior of a fin-tube heat exchanger. *International Journal of Refrigeration* 25: 1047–53. [https://doi.org/10.1016/S0140-7007\(02\)00008-7](https://doi.org/10.1016/S0140-7007(02)00008-7). <http://www.sciencedirect.com/science/article/pii/S0140700702000087>.
- Jiang, Y., H. Fu, Y. Yao, L. Yan, and Q. Gao. 2014. Experimental study on concentration change of spray solution used for a novel non-frosting air source heat pump system. *Energy and Buildings* 68: 707–12. <https://doi.org/10.1016/j.enbuild.2013.08.055>. <http://www.sciencedirect.com/science/article/pii/S0378778813005525>.
- Jin, L., F. Cao, D. Yang, and X. Wang. 2016. Performance investigations of an R404A air-source heat pump with an internal heat exchanger for residential heating in Northern China. *International Journal of Refrigeration* 67: 239–48. <https://doi.org/10.1016/j.ijrefrig.2016.03.004>. <http://www.sciencedirect.com/science/article/pii/S0140700716300093>.
- Kamel, R. S., and A. S. Fung. 2014. Modeling, simulation and feasibility analysis of residential BIPV/T + ASHP system in cold climate—Canada. *Energy and Buildings* 82: 758–70. <https://doi.org/10.1016/j.enbuild.2014.07.081>. <http://www.sciencedirect.com/science/article/pii/S0378778814006306>.
- Laref, R., E. Losson, A. Sava, and M. Siadat. 2019. On the optimization of the support vector machine regression hyperparameters setting for gas sensors array applications. *Chemometrics and Intelligent Laboratory Systems* 184: 22–7. <https://doi.org/10.1016/j.chemolab.2018.11.011>. <http://www.sciencedirect.com/science/article/pii/S0169743918303010>.
- Li, B., P. Wild, and A. Rowe. 2019. Performance of a heat recovery ventilator coupled with an air-to-air heat pump for residential suites in Canadian cities. *Journal of Building Engineering* 21: 343–54. <https://doi.org/10.1016/j.jobte.2018.10.025>. <http://www.sciencedirect.com/science/article/pii/S2352710218305448>.
- Li, Q., Q. Meng, J. Cai, H. Yoshino, and A. Mochida. 2009. Applying support vector machine to predict hourly cooling load in the building. *Applied Energy* 86: 2249–56. <https://doi.org/10.1016/j.apenergy.2008.11.035>. <http://www.sciencedirect.com/science/article/pii/S0306261908003176>.
- Li, Y., W. Li, Z. Liu, J. Lu, L. Zeng, L. Yang, and L. Xie. 2017. Theoretical and numerical study on performance of the air-source heat pump system in Tibet. *Renewable Energy* 114: 489–501. <https://doi.org/10.1016/j.renene.2017.07.036>. <http://www.sciencedirect.com/science/article/pii/S0960148117306493>.
- Liu, F., L. Wang, Q. Wang, and H. Wang. 2017. Experiment study on heating performance of solar-air source heat pump unit. *Procedia Engineering* 205: 3873–8. <https://doi.org/10.1016/j.proeng.2017.10.054>. <http://www.sciencedirect.com/science/article/pii/S1877705817346040>.
- Long, J., R. Zhang, J. Lu, and F. Xu. 2019. Heat transfer performance of an integrated solar-air source heat pump evaporator. *Energy Conversion and Management* 184: 626–35. <https://doi.org/10.1016/j.enconman.2019.01.094>. <http://www.sciencedirect.com/science/article/pii/S0196890419301487>.
- Luo, X., Q. Hou, Y. Wang, D. Xin, H. Gao, M. Zhao, and Z. Gu. 2017. Experimental on a novel solar energy heating system for residential buildings in cold zone of China. *Procedia Engineering* 205: 3061–6. <https://doi.org/10.1016/j.proeng.2017.10.282>. <http://www.sciencedirect.com/science/article/pii/S1877705817349421>.

- Ma, Z., C. Ye, and W. Ma. 2019. Support vector regression for predicting building energy consumption in Southern China. *Energy Procedia* 158: 3433–8. <https://doi.org/10.1016/j.egypro.2019.01.931>. <http://www.sciencedirect.com/science/article/pii/S1876610219309762>.
- Mascher, S. 2018. Striving for equivalency across the Alberta, British Columbia, Ontario and Québec carbon pricing systems: The pan-Canadian carbon pricing benchmark. *Climate Policy* 18 (8): 1012–27. doi:<https://doi.org/10.1080/14693062.2018.1470489>
- National Energy Board. 2020. NEB – provincial and territorial energy profiles – Canada. Accessed February 20, 2020. <https://www.cer-rec.gc.ca/nrg/ntgrtd/mrkt/nrgsstmprfls/cda-eng.html>.
- National Research Council of Canada. 2017. *National energy code of Canada for buildings 2017*. 4th ed. Ottawa: National Research Council of Canada.
- Natural Resources Canada. 2016. Total end-use sector - energy use analysis. Government of Canada. <http://oee.nrcan.gc.ca/corporate/statistics/neud/dpa/showTable.cfm?type=AN&sector=aaa&juris=ca&m=1&page=0>.
- Parveen, N., S. Zaidi, and M. Danish. 2019. Support Vector Regression (SVR)-based adsorption model for Ni (II) ions removal. *Groundwater for Sustainable Development* 9: 100232. <https://doi.org/10.1016/j.gsd.2019.100232>. <http://www.sciencedirect.com/science/article/pii/S2352801X18301024>.
- Rylan Urban. 2020. Electricity prices in Canada (Updated 2019). Rylan Urban. Accessed February 13, 2020. <https://energyhub.org/electricity-prices/>.
- Song, M., G. Gong, N. Mao, S. Deng, and Z. Wang. 2017. Experimental investigation on an air source heat pump unit with a three-circuit outdoor coil for its reverse cycle defrosting termination temperature. *Applied Energy* 204: 1388–98. <https://doi.org/10.1016/j.apenergy.2017.01.068>. <http://www.sciencedirect.com/science/article/pii/S0306261917300806>.
- Song, M., N. Mao, S. Deng, Y. Xia, and Y. Chen. 2016. An experimental study on defrosting performance for an air source heat pump unit at different frosting evenness values with melted frost local drainage. *Applied Thermal Engineering* 99: 730–40. <https://doi.org/10.1016/j.applthermaleng.2015.12.100>. <http://www.sciencedirect.com/science/article/pii/S1359431115015033>.
- Statistics Canada. 2017. Canadian monthly natural gas distribution, Canada and provinces (X 1,000). Statistics Canada. <https://www150.statcan.gc.ca/t1/tb1/en/tv.action?pid=2510005901>.
- Statistics Canada. 2020a. Census Profile, 2016 Census. Statistics Canada. <https://www12.statcan.gc.ca/census-recensement/2016/dp-pd/prof/index.cfm?Lang=E>.
- Statistics Canada. 2020b. Monthly average retail prices for gasoline and fuel oil, by geography. Statistics Canada. <https://www150.statcan.gc.ca/t1/tb1/en/tv.action?pid=1810000101>.
- Swan, L. G., V. I. Ugursal, and I. Beausoleil-Morrison. 2009. A database of house descriptions representative of the Canadian housing stock for coupling to building energy performance simulation. *Journal of Building Performance Simulation* 2 (2): 75–84. doi:<https://doi.org/10.1080/19401490802491827>
- Thomas, W. D., and J. J. Duffy. 2013. Energy performance of net-zero and near net-zero energy homes in New England. *Energy and Buildings* 67: 551–8. <https://doi.org/10.1016/j.enbuild.2013.08.047>. <http://www.sciencedirect.com/science/article/pii/S0378778813005446>.
- Udovichenko, A., and L. Zhong. 2019. Application of Air-Source Heat Pump (ASHP) technology for residential buildings in Canada. *IOP Conference Series: Materials Science and Engineering* 609: 52006. doi:<http://dx.doi.org/10.1088/1757-899X/609/5/052006>
- Vapnik, V., S. E. Golowich, and A. J. Smola. 1997. Support vector method for function approximation, regression estimation and signal processing. In *Advances in neural information processing systems 9*, ed. M. C. Mozer, M. I. Jordan and T. Petsche, 281–7. Cambridge: MIT Press. <http://papers.nips.cc/paper/1187-support-vector-method-for-function-approximation-regression-estimation-and-signal-processing.pdf>.
- Wang, R., S. Lu, and Q. Li. 2019. Multi-criteria comprehensive study on predictive algorithm of hourly heating energy consumption for residential buildings. *Sustainable Cities and Society* 49: 101623. <https://doi.org/10.1016/j.scs.2019.101623>. <http://www.sciencedirect.com/science/article/pii/S2210670719309527>.
- Wang, W., Y. C. Feng, J. H. Zhu, L. T. Li, Q. C. Guo, and W. P. Lu. 2013. Performances of air source heat pump system for a kind of mal-defrost phenomenon appearing in moderate climate conditions. *Applied Energy* 112: 1138–45. <https://doi.org/10.1016/j.apenergy.2012.12.054>. <http://www.sciencedirect.com/science/article/pii/S0306261912009452>.
- Wang, Z., F. Wang, Z. Ma, M. Song, and W. Fan. 2018. Experimental performance analysis and evaluation of a novel frost-free air source heat pump system. *Energy and Buildings* 175: 69–77. <https://doi.org/10.1016/j.enbuild.2018.07.031>. <http://www.sciencedirect.com/science/article/pii/S0378778818314300>.
- Wang, Z., F. Wang, X. Wang, Z. Ma, X. Wu, and M. Song. 2017. Dynamic character investigation and optimization of a novel air-source heat pump system. *Applied Thermal Engineering* 111: 122–33. <https://doi.org/10.1016/j.applthermaleng.2016.09.076>. <http://www.sciencedirect.com/science/article/pii/S1359431116316842>.
- Weis, T., B. Thibault, and B. Miller. 2016. Chapter 15: Alberta's electricity future. In *First world petro-politics: The political ecology and governance of Alberta*, ed. Laurie Adkin. Toronto: University of Toronto Press.
- Xuan, Z., Z. Xuehui, L. Liequan, F. Zubing, Y. Junwei, and P. Dongmei. 2019. Forecasting performance comparison of two hybrid machine learning models for cooling load of a large-scale commercial building. *Journal of Building Engineering* 21: 64–73. <https://doi.org/10.1016/j.jobe.2018.10.006>. <http://www.sciencedirect.com/science/article/pii/S2352710218307101>.
- Yao, Y., Y. Jiang, S. Deng, and Z. Ma. 2004. A study on the performance of the airside heat exchanger under frosting in an air source heat pump water heater/chiller unit. *Journal of Heat and Mass Transfer* 47: 3745–56. <https://doi.org/10.1016/j.ijheatmasstransfer.2004.03.013>. <http://www.sciencedirect.com/science/article/pii/S0017931004001097>.
- Zhang, D., J. Li, J. Nan, and L. Wang. 2016. Thermal performance prediction and analysis on the economized vapor injection air-source heat pump in cold climate region of China. *Sustainable Energy Technologies and Assessments* 18: 127–33. <https://doi.org/10.1016/j.seta.2016.10.008>. <http://www.sciencedirect.com/science/article/pii/S2213138816301321>.
- Zhang, L., T. Fujinawa, and M. Saikawa. 2012. A new method for preventing air-source heat pump water heaters from frosting. *International Journal of Refrigeration* 35: 1327–34. <https://doi.org/10.1016/j.ijrefrig.2012.04.004>. <http://www.sciencedirect.com/science/article/pii/S0140700712000850>.
- Zhang, L., Y. Jiang, J. Dong, and Y. Yao. 2018. Advances in vapor compression air source heat pump system in cold regions: A review. *Renewable and Sustainable Energy Reviews* 81: 353–65. <https://doi.org/10.1016/j.rser.2017.08.009>. <http://www.sciencedirect.com/science/article/pii/S1364032117311401>.